Journal of Hydrology 595 (2021) 126047

Contents lists available at ScienceDirect

Journal of Hydrology

journal homepage: www.elsevier.com/locate/jhydrol

Research papers

Disentangling the effect of future land use strategies and climate change on streamflow in a Mediterranean catchment dominated by tree plantations

Mauricio Galleguillos [a,b,*], Fernando Gimeno [a,b], Cristóbal Puelma [a,b], Mauricio Zambrano-Bigiarini [b,c], Antonio Lara [b,d,e], Maisa Rojas [b,e,f]

[a] Department of Environmental Science and Renewable Natural Resources, University of Chile, Santiago, Chile
[b] Center for Climate and Resilience Research (CR2), University of Chile, Santiago, Chile
[c] Department of Civil Engineering, Universidad de La Frontera, Temuco, Chile
[d] Instituto de Conservación, Biodiversidad y Territorio, Universidad Austral de Chile, Valdivia, Chile
[e] Fundación Centro de los Bosques Nativos FORECOS, Valdivia, Chile
[f] Department of Geophysics, University of Chile, Santiago, Chile

ARTICLE INFO

This manuscript was handled by marco borga, Editor-in-Chief.

Keywords:
LULCC
Exotic plantations
Native shrubland
SWAT
Hydrological response
SDGs

ABSTRACT

Climate change (CC) along with Land Use and Land Cover Change (LULCC) have a strong influence in water availability in already fragile Mediterranean ecosystems. In this work the Soil and Water Assessment Tool (SWAT) was implemented for the 2006–2018 period in a rainfed catchment of central Chile (36°) to test the hypothesis that adaptive plantation strategies could mitigate the impacts of climate change and increase streamflow. We also hypothesize that afforestation with exotic tree plantations will reduce water availability in Mediterranean catchments, acting in synergy with climate change. Five LULCC scenarios are analyzed: i) current long-term national Forest Policy (FP), ii) extreme scenario (EX) with large afforestation surfaces, both including the replacement of native shrublands with *Pinus radiata*; iii) adaptive plantation management scenario (FM), with lower planting density, iv) forced land displacement scenario (FLD), where plantations at the headwaters are moved to lowland areas and replaced with native shrublands, and v) pristine scenario (PR), with only native vegetation. Each LULCC scenario was run with present climate and with projections of different CMIP5 climate models under the RCP 8.5 scenario for the period 2037–2050, and then compared against simulations based on the present land cover and climate. Simulations with the five LULCC scenarios (FP, EX, FM, FLD and PR) with present climate resulted in variations of −2.5, −17.3, 0, 2.3 and 10.9% on mean annual streamflow (Q), while simulations with the current land cover and CC projections produced a 32.1% decrease in mean annual Q. The joint impact of CC and LULCC leads to changes in mean annual Q ranging from −46.2% (EX) to −23.3% (PR). Afforestation with exotic pines will intensify the reduction in water yield, while conservative scenarios focused on native forests protection and restoration could partially mitigate the effect of CC. We make a strong call to rethink current and future land management strategies to cope with lower water availability in a drier future.

1. Introduction

Societies already affected by water scarcity are struggling to devise effective ways to mitigate the negative impacts of global change on water availability, both for human beings and ecosystems (Rossing, 2010). Mediterranean regions are particularly prone to droughts given observed and projected reduction of precipitation due to climate change (CC) (Polade et al., 2017; Rojas et al., 2019). Central Chile (30-39°S) has undergone a negative precipitation trend of approximately 4% per decade between 1960 and 2016 (Boisier et al, 2018), accompanied by an increase in air temperature of about 0.18 °C/decade for the Central Depression for the 1979–2006 period (Falvey and Garreaud, 2009). The current decade is the warmest of the last 100 years, and during the last nine years, the so called Chilean megadrought stands out as the longest and most extended dry period on record, causing higher evaporation rates in water bodies, larger evapotranspiration (ET) from crops and natural vegetation, and an accelerated melting of snow. The hydrological response of catchments has also been affected, causing an important reduction in streamflow (Q), and shortages on drinking water for rural communities (Alvarez-Garreton et al., 2018; Garreaud et al., 2017). A

* Corresponding author at: Department of Environmental Science and Renewable Natural Resources, University of Chile, Santiago, Chile.
E-mail address: mgalleguillos@renare.uchile.cl (M. Galleguillos).

https://doi.org/10.1016/j.jhydrol.2021.126047

Available online 5 February 2021

more severe effect is expected in the near future, with projected reductions in precipitation of up to 30%, leading to runoff reductions of about 40% under RCP8.5 (Bozkurt et al., 2018; Valdés-Pineda et al., 2014).

Land use and land cover change (LULCC) is the other main driver of global change, with important impacts at global and local scale. One of the most important changes in land use is afforestation with commercial exotic tree plantations, which increased from 167.5 to 277.9 million hectares worldwide between 1990 and 2015. Temperate zones (such as Mediterranean regions) represent 56% of this area (Payn et al, 2015). South America is currently experiencing the rapid expansion of exotic species of commercial tree plantations (Jones et al., 2016). In particular, Chile stands out as the fifth largest producer of roundwood in the world, on the basis of fast-growing monoculture plantations of *Pinus radiata* and *Eucalyptus* spp. with (short) rotations of 18 and 10–12 years, respectively (Jürgensen et al., 2014). This timber industry is the second largest commercial export sector in Chile after mining (Salas et al., 2016), and it was consolidated in mid-1970′s with the implementation of state subsidies to encourage private sector participation in the expansion of forest plantations as a basis for the development of the private forest industry and exportations (Lara & Veblen 1993). Thus, planted area grew from 375,000 to 1.7 million hectares between 1970 and 1994 (Niklitschek, 2007), and to 2.3 million hectares in 2015 (INFOR, 2015), concentrated mainly in the area located between 34° and 41°S, specifically in the coastal mountain range (Armesto et al., 2010). This area is intended to increase under the current 2015–2035 Chilean Forest Policy to contribute to the country's economic and social development (MINAGRI, 2015). Absorption and sequestration of CO2 by forests also play a significant role in Chile's commitment to carbon neutrality by 2050, and is part of the country's Nationally Determined Contributions (NDC), to fullfil international climate commitments defined in the ratification of the Paris Agreement (Government of Chile, 2020).

Worldwide, several studies support the hypothesis of a strong negative impact of forest plantations on water yield when they replace other covers (e.g., grasslands, shrublands), since they modify transpiration, interception and evaporation processes within a catchment (Calder, 2007; Farley et al., 2005; Garmendia et al, 2012; Zhang et al., 2011, 2017). In Chile, some studies highlight this evidence at different scales: in experimental plots and small-scale catchments, forest plantations have been associated with higher consumption of soil water compared to grasslands, producing high ET rates and low percolation (Huber et al., 2008). *P. radiata* plantations have been related to the high interception of canopy precipitation, while actual ET is fed exclusively by edaphic water during summer (Huber et al., 2010). Consistent results were obtained using satellite observations through an energy balance model over a landscape of south-central Chile, where forest plantations showed higher ET rates during spring (Olivera-Guerra et al., 2014). In addition, Lara et al. (2009) reported a negative correlation between (annual and summer) runoff and the forest plantation area in small coastal catchments of southern Chile (*c.* 40° S), while a positive correlation was found between runoff and the area of native forest cover during the dry season. At a larger scale, a decrease in summer runoff was reported in response to the increase in the area of *P. radiata* plantations at the expense of native forest in the period 1975–2000 in two catchments of south-central Chile (252 and 650 km^2) (Little et al., 2009). In southern catchments of similar size, decreasing flows during summer were found when afforestation was introduced using a statistical model (Iroumé & Palacios, 2013). Recently, a study comprising 25 large forested catchments in south-central Chile showed a general decrease in Q when shrublands, pastures or native forest are replaced by exotic forest plantations, using a statistical regression between precipitation and spatially distributed land cover data (Alvarez-Garreton et al., 2019).

On the other hand, there is a wide range of studies that analyze changes in the hydrological cycle due to changes in land cover and/or climate (Garmendia et al., 2012; Lu et al., 2015; Molina-Navarro et al., 2016; Stehr et al., 2010), which have provided useful insights for water resources management (Gassman et al., 2014). However, only few studies (Serpa et al., 2015; Carvalho-Santos et al., 2016) proposed to disentangle the joint effect of CC and LULLC, especially on the hydrological regime of Mediterranean forested catchments. Process-based hydrological models are some of the tools commonly used to evaluate changes in individual components of the hydrological cycle (Devia et al., 2015). The Soil and Water Assessment Tool (SWAT) model was developed to predict the impact of land management practices and their use on water resources in large and complex catchments, considering different soil types, land use, topography and management practices (Arnold et al., 2012).

This research aims to provide evidence for policy recommendations on land management strategies required to cope with lower water availability in Mediterranean catchments where tree plantation afforestation is under discussion. We hypothesize that adaptive plantation strategies could mitigate the impacts of climate change and increase streamflows. Additionally, we hypothesize that afforestation with exotic tree plantations will reduce water availability in the Mediterranean catchments, acting in synergy with climate change. To test these hypotheses, we selected the Cauquenes catchment (620 km^2), located in the Mediterranean south-central Chile, as a case study. This catchment was selected because large areas of native vegetation have been replaced by exotic tree plantations in the last decades, and the current Chilean Forest Policy threatens to exacerbate this trend. In addition, this catchment is highly vulnerable to the impacts of climate change, due to high poverty (Pino et al., 2015), and the presence of native ecosystems in danger of extinction (Alaniz et al., 2016). Hence decision on future land use change should consider addressing several objectives at the same time, as is the call under the UN 2030 Agenda of the Sustainable Development Goals (SDGs).

2. Methodology

The general framework of the methodology is displayed in Fig. 1, where we can distinguished four main themes: i) The SWAT implementation (center), with a general description of the hydrological modelling procedure (e.g. calibration method); ii) the CC and LULCC scenarios (upper and lower part of the figure); iii) analysis of SWAT simulations of spatio-temporal patterns of three hydrological components (to the left), considering the Hydrological Response Units (HRUs) behavior during dry and normal years under present and CC periods; iv) analysis of the relative differences of Qs between the present condition and the five LULCC; the 24 CC-models; and the joint effect of LULCC and CC-scenarios (to the right).

2.1. Study area

The study area corresponds to the headwaters of the Cauquenes River catchment (620 km^2), a tributary of the Maule river, located on the eastern slope of the Coastal mountain range in south-central Chile (Fig. 2). This catchment has a warm-summer Mediterranean climate (Csb) in the Köppen-Geiger classification, and it is water-limited according to Budyko's dryness index (Mcvicar et al., 2012). The annual precipitation is 814 mm, concentrated from April to September, with strong inter-annual variability, while the annual average temperature is 14.7 °C according to a historical weather station located downstream with records since 1976. The catchment has no nival contribution, so its hydrological regime is strictly rainfed, with the highest flows during winter (JJA), and the lowest water levels during summer (DJF). In July, streamflows reach values above 20 m^3 s^{-1} 50% of the time, while during summer 100% of the time streamflows are below 2 m^3 s^{-1}. Elevation ranges from 150 to 750 m a.s.l., with an average of 317 m a.s.l. and an average slope of 17% (Fig. 2a). The catchment provides ideal conditions to study the effect of land use on different components of the hydrological cycle for two main reasons: i) irrigation can be neglected, since the anthropogenic activities are mainly rainfed crops or forest

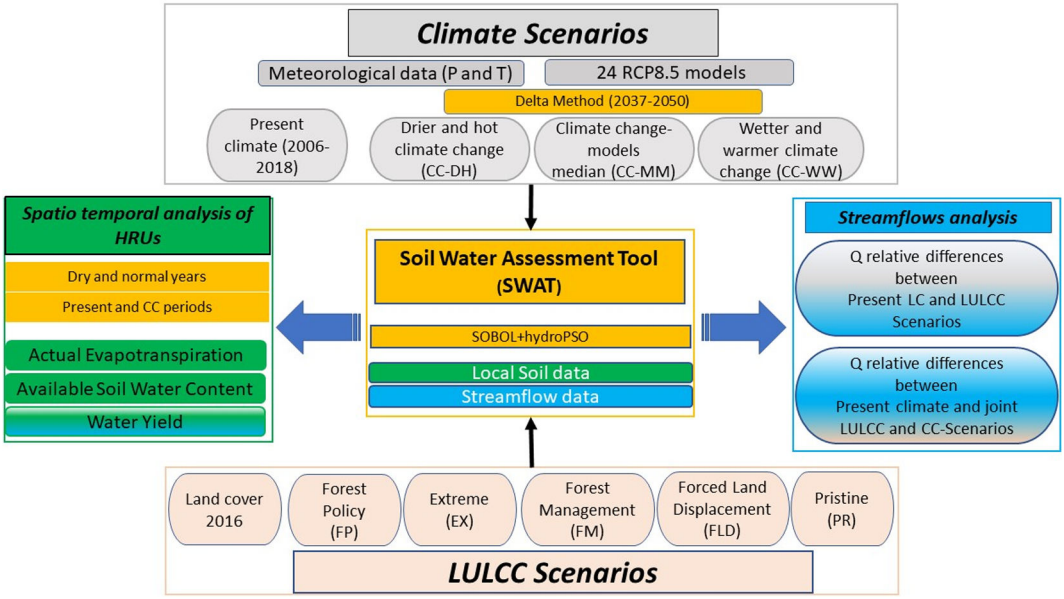

Fig. 1. Methodological scheme of assessment of global change impacts on catchment streamflows.

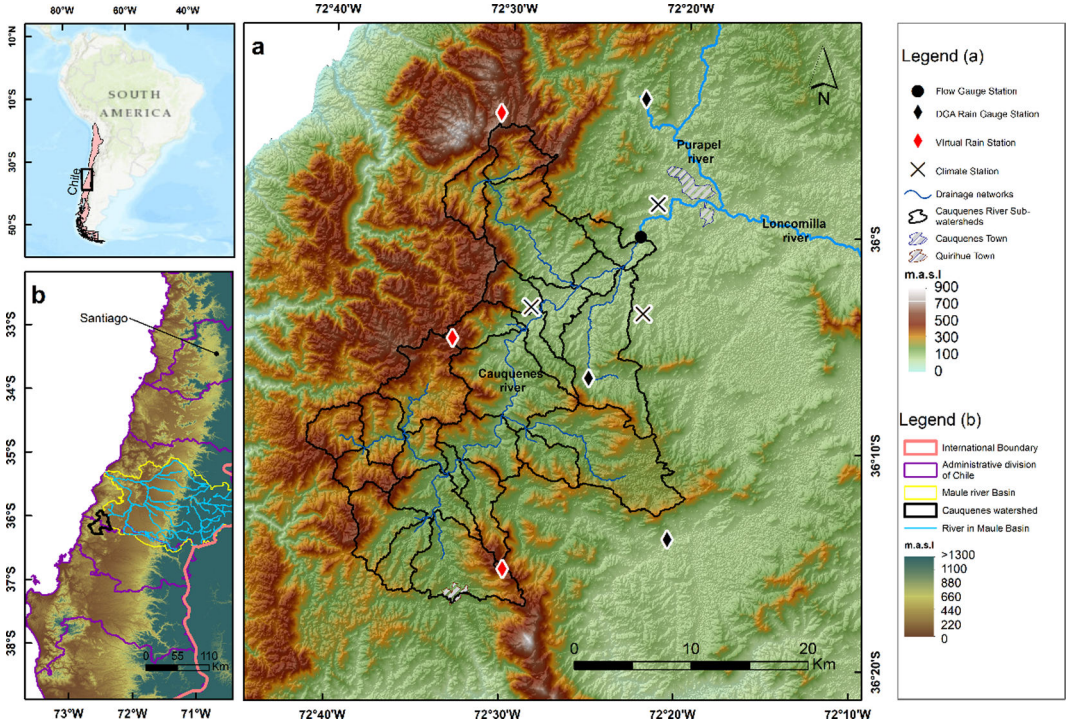

Fig. 2. Study Area. (a): Topography of South-Central Chile with the Maule River Basin displayed (b): Cauquenes catchment with the subcatchments defined by SWAT. Drainage network, meteorological stations, streamflow station and urban areas are also depicted.

plantations; ii) it has little hydraulic infrastructure, such as irrigation channels and reservoirs; and iii) it has a mosaic of land use classes with different water consumption rates, which can be used for evaluating LULCC impacts on Q. It is important to note that the downstream area of the Cauquenes river is of utmost importance for human activities such as agriculture, recreational purposes and drinking water for rural and urban areas.

2.2. The SWAT model

The Soil and Water Assessment Tool (SWAT) is a process-based, catchment scale semi-distributed hydrological model. In SWAT each sub-catchment is divided into hydrological response units (HRUs), which consists of homogeneous areas in terms of soil type, land cover, slope and water management practices (Neitsch et al., 2011). In this work HRUs representative of the two main land cover types (native shrublands and exotic forest plantations) are used to study the evolution of individual components of the hydrological cycle (precipitation, actual evapotranspiration and water yield). Surface runoff is estimated with the modified "SCS curve number" method, while potential ET was computed with the Hargreaves equation, both chosen based on input data availability. The variable storage method was selected to route

water through the drainage network. For further details of the equations used to represent hydrological processes, see the theoretical documentation of the model in Neitsch et al., (2011). The QSWAT software was used as an interface (Dile et al., 2016) to prepare the input data used to run SWAT 2012 rev637.

2.3. Input data

2.3.1. Topography and catchment delineation

We used the 12.5 m TanDem-X Digital Elevation Model of the German Aerospace Center and EADS Astrium. To define the subcatchments, we used the Strahler method with a threshold of 12.5 km^2 to define the minimum drainage area, resulting in 26 subcatchments. HRUs are obtained considering slope bands of 10, 20, 30 and > 30%, and a minimum size of 2.5% of the corresponding subcatchments, resulting in 233 HRUs.

2.3.2. Land use land cover data

Land cover was generated using a supervised classification based on Landsat OLI satellite data for February 2016, following the methodology of Chuvieco (2008). The overall accuracy (OA) was 86.5% and the Kappa coefficient was 0.81, considered almost perfect (Landis & Koch, 1977). The largest uncertainty corresponded to agriculture and pasturelands with baren areas, which were confused by the classifier with shrublands. A 7x7 filter and a 3x3 grouping were applied, reallocating isolated and anomalous pixels to achieve a sharper spatial distribution of the categories. Then, the classified land covers were assigned to existing vegetation categories in SWAT according to Table 1. The area covered by the different land use/land cover classes are: forest plantations (43%), shrublands (43%), barren areas (including clearcuts) (10%), native forests (3%), urban areas (town of Quirihue 0.5%) located in the southern portion of the catchment, and agriculture and pasturelands (0.4%) (Fig. 3).

2.3.3. Soil data

Soils of Cauquenes are classified as lithosols (I-Lc.c) (CIREN, 1997), and soil data was available as orthophotos at a 1:20,000 scale. In addition, we introduced physical properties measured in situ from the database of Soto et al., (2019) (details of the data in Supplementary material I) following Chen et al. (2016). Soil depth was fixed to 2 m for all land uses, based on the average depth of the catchment according to global gridded soil information (Hengl et al., 2017), but *P. radiata* plantations and native forest were fixed to 3 m according to their capabilities to extract water from deeper horizons (Sand & Nambiar, 1984; Teskey & Sheriff, 1996; Huber et al., 2010).

2.3.4. Climate data

Daily precipitation (P) and air temperature were obtained from three rain gauges, three weather stations from public institutions for the 2006–2018 period and three rain gauges located in high elevation for the 2018–2019 period (Fig. 2 and Supplementary material II). For each subcatchment, SWAT uses the closest climate and rain gauge station. Quality assessment of P data was performed using a double-mass curve analysis. Gap filling was done using regressions with the nearest station (less than 3% of missing data). For temperature, an exploratory analysis was used to verify anomalous data, while gap filling was performed with linear regression with the nearest station (on average less than 10% of missing data). Three virtual rain gauges were included to represent topographic effect, as previously reported for Chilean coastal range (Garreaud et al., 2016). The daily 5-km resolution CR2MET precipitation dataset (http://www.cr2.cl/datos-productos-grillados), was used to provide three virtual rain gauges to represent high elevation rainfall. This product was verified according to a point-to-pixel analysis against three rain gauge stations (HOBO Rain Gauge RG3-5) installed during the 2018–2019 period (Supplementary material II). Satisfactory results were obtained, with correlations ranging from 0.6 to 0.68 at daily scale and 0.93 to 0.98 at monthly scale.

2.3.5. River discharge data

Daily observations were obtained from the "Río Cauquenes en el Arrayán" discharge station (Supplementary material II). Gap filling was not performed (it has 95% data in the period). In addition, possible anthropogenic modifications to the measurements and data consistency were verified through the method of double-mass curves with two streamflow stations: Río Cauquenes en Desembocadura (35° 54'S, '72° 03'O) and Río Purapel en Sauzal (35° 45'S, 72° 04 'W).

2.4. Model implementation

Thirteen years of simulation period was chosen (2006–2018) for flow evaluation when land use changes are modified. This period represents a compromise between a sufficient extensive time series of streamflow data and the stable landscape of the catchment represented by the current land cover reference scenario. The model was run at the daily time step, using 2006–2007 and 2008–2014 as warming up and calibration periods, respectively. The verification period considered years 2015 to 2018.

2.4.1. Parameter identification

To reduce the number of parameters to be calibrated, a sensitivity analysis was carried out for 15 parameters selected based on literature review. The sensitivity analysis was carried out using a variance-based global sensibility analysis technique (Sobol) (Sobol, 2001; Saltelli et al., 2010). This method provides an efficient and effective way to assess parameter sensitivity across a full range of parameter values. Model parameters were selected to represent the following hydrological processes: runoff (CN2, CH_N (1), SURLAG and OV_N); groundwater (GW_DELAY, RCHRG_DP, GWQMN, ALPHA_BF, REVAPMN and GW_REVAP); evapotranspiration (EPCO and ESCO); and water routing (CH_N (2), CH_K (2), ALPHA_BNK). Physical ranges used for the

Table 1
Description of the land cover / uses present in the watershed based on the supervised classification. Land cover names and equivalent code are presented in SWAT, its area in km^2 and its% with respect to the catchment.

Land Cover	Field description	SWAT cover name	SWAT code	area km^2	area %
Barren areas	Zone without vegetation	Barren	BARR	68.17	11
Native Forests	Deciduous forest of *Nothofagus glauca* and *N. obliqua*	Oak	OAK	16.67	2.69
Agriculture and pasturelands	Cutivated zones, natural and managed pasturelands	Dryland, cropland and pastures	CRDY	2.96	0.48
Forest Plantations	Forest Plantations, mainly *Pinus radiata*	Forest evergreen	FRSE	265.96	42.91
Shrublands	Scaterred bush vegetation (25–50% cover) *Acacia caven*, *Baccharis sp*, *Schinus polygamus* and species of sclerophyll forest such as *Quillaja saponaria* y *Lithrea caustica*	Shrubland	SHRB	264.44	42.66
Urban	Urban land with medium density	Urban medium density	URML	1.62	0.26
Total				619.81	100

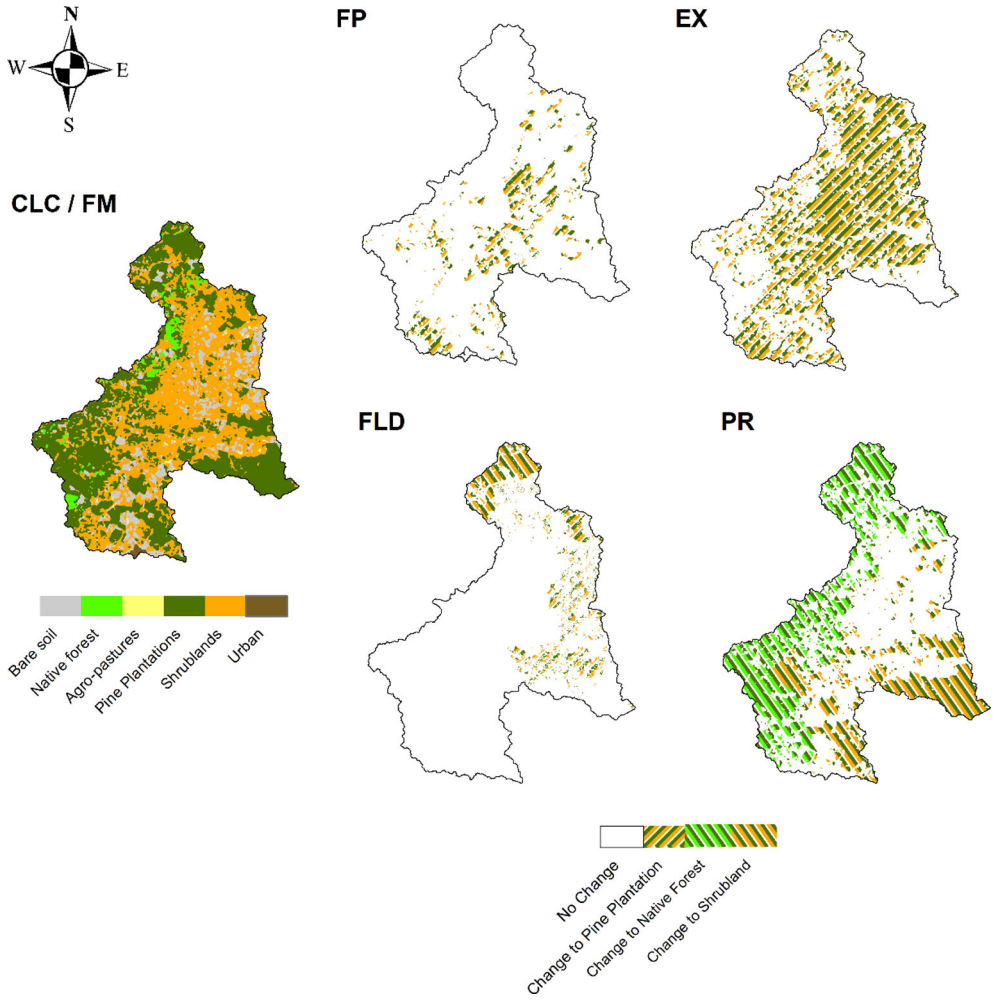

Fig. 3. Spatial representation of Land Use and Land Cover scenarios: current land cover with actual management (2016) (CLC); and under a less intensive forest management (FM); forest policy 2015–2035 (FP); extreme expansion of forest plantations (EX); forced land displacement of plantations from headwaters (FLD); and restoration strategy with native vegetation (PR).

sensitivity analysis were obtained from the SWAT manual (Arnold et al., 2012; Neitsch et al., 2011), with the exception of SURLAG, GW_DELAY, and REVAPMN, which ranges were obtained from Brown et al. (2015); Heathman et al. (2009); Stehr et al. (2010); Van Liew et al., (2007). The meaning of the parameters is explained in the Supplementary material III.

2.4.2. *Vegetation parameters*

The management and phenological cycle of Forests Plantations (FRSE) and Shrublands (SHRB) were represented with parameters obtained from the literature for similar local conditions obtained, as described in (Table 2).

2.4.3. *Calibration and verification*

Calibration process was carried out with the default configuration of hydroPSO global optimization algorithm (Zambrano-Bigiarini & Rojas, 2013), using the Nash-Sutcliffe goodness-of-fit index (NSE) as objective function. The Nash-Sutcliffe efficiency (NSE), the percentage of bias (Pbias), and the ratio between the mean square error and the standard deviation of the data (RSR) were used as goodness of fit measures for calibration and verification. In general, monthly simulations are considered satisfactory when they satisfy: NSE > 0.50, RSR < 0.70, and PBIAS $= \pm$ 25% (Moriasi et al., 2007).

Table 2
Crop modified parameters. In brackets the default SWAT value is shown and on the left the modified values based on the literature: [1](Álvarez et al., 2012); [2] (Raab et al., 2015); [3] (Rook & Corson, 1978); [4] The growth range is very wide and varied, however 14° was used since at this average temperature new shoots were observed in the bushes (in the field); [5] (Ovalle, et al., 1990).

CPNM	CROPNAME	BLAI	FRGRW2	CHTMX	T_BASE	ALAI_MIN
FRSE	Forest-Evergreen	3.7[1] (4)	0.5 (0.25)	20 (10)	10[3] (0)	2.5[1] (0.75)
SHRB	Shrublands	1.6 (2)	0.25	2[5](1)	14[4] (12)	0.2[2] (0)

CPNM is a code to represent the land cover/plant name in SWAT; CROPNAME is the crop name in SWAT; BLAI is the Maximum potential leaf area index; FRGRW2 is Fraction of the plant growing season; CHTMX is Maximum canopy height in meters; T_BASE is the maximum base temperature for plant growth in °C and ALAI_MIN is Minimum leaf area index for plant during dormant period (m^2m^{-2}).

2.5. Global change scenarios

2.5.1. Land use change scenarios

Six LULCC scenarios are analyzed (Fig. 3 and Table 3): the current land cover (CLC); two describing an increase in forest plantation area (FP, EX); one emulating a forest plantation management strategy (FM); and two conservative scenarios (FLD, PR). The effect of these scenarios on Q are analyzed for present and future CC periods. These scenarios represent the whole range of possible land cover modifications in the catchment and are described in the following paragraphs.

- **Forest Policy Scenario (FP)**: This scenario represents one of the goals of the strategic axis "Productivity and economic growth" of Chilean government, where afforestation of half a million of hectares, preferably in forestry land belonging to small and medium-size owners, has to be done by 2035 without replacing native forest (MINAGRI, 2015). Low-quality soils available to establish forest plantations were identified based on the soil aptitude map of CIREN (1997). The small and medium-sized owners (200 ha or less) were identified with the cadastral map of rural properties CIREN (2001). The current land cover map (2016) was used to identify all the areas covered by shrublands, which were selected as the non-native forest land cover to be transformed into exotic forest plantations, keeping all other coverage constant. Finally, a unique map was generated that integrates the previous criteria of land use modification through map algebra performed in QGIS 2.6. 9.8% of the current shrubland land cover that fulfill the three criteria described before were converted to *P. radiata* plantations.
- **Extreme Scenario (EX)**: This scenario represents the replacement of all the existing native shrublands with exotic forest plantations. We decided to include this extreme scenario given the current discussion about Chile's strategies to fulfill the NDC's commitments (Government of Chile, 2020), with massive afforestation being discussed as a possibility. Although this scenario seems extreme, a similar transformation already occurred in the past, when the national forest policy, afforestation subsidies, and the expansion of the forest industry increased the surface planted with exotic trees in the region exponentially (Echeverria et al., 2006). In addition, shrubland ecosystems do not have a protection law that can avoid their conversion into forest plantations (Alaniz et al., 2016). The total area of shrubland (42.7% of the catchment) was converted to plantation.
- **Present land use with Forest Management (FM)**: This scenario represents a CC adaptation strategy, where forestry companies use a less intensive forest stand management to address current and projected water scarcity. To emulate this situation, we maintained the current land cover area but with lower density of tree plantations, reducing the maximum leaf area index (LAI) in the SWAT model. We proposed a LAImax = 3.1 (instead of 3.7) calculated by subtracting 60% of the standard deviation of LAI measurements obtained from 13*P. radiata* plots under similar site conditions described in Álvarez et al. (2012).
- **Forced Land Displacement (FLD)**: This CC adaptation strategy is analyzed to protect water yield as a key ecosystem service. In this scenario exotic plantations are moved from headwaters into lower land areas, as an ecological strategy leaving their original area to be replaced by native shrublands. This scenario considered natural regeneration of vegetation and is likely probable that shrublands will be established in the 2037–2050 period because future CC conditions would limit the development of actual native forest, in terms of structure and composition, due to its low rate of growth, the increase of stressors like droughts, change of seasonal phenology, and insect herbivory (Xie et al., 2015; Yu et al., 2016; Estay et al., 2019; Huang et al., 2020). The scenario considered natural regeneration of vegetation and according to ecological conditions is likely to similar scenarios have been proposed by other studies to quantify the effect of a technocratic-like political decision into the provision of an ecosystem service (Manuschevich et al., 2019). 2800 ha of *P. radiata* were displaced to lowlands and were replaced by shrublands from the lowland area.
- **Pristine Native Vegetation (PR)**: This scenario replaces all the current exotic forest plantations with native forest and shrublands, as part of a massive ecological restoration strategy to protect local endangered biodiversity. It is created using the potential native vegetation belt proposed by Luebert and Pliscoff (2018) as the maximum area to represent the potential area cover by native forest and shrubland. Three vegetation belts are described for the catchment, the deciduous forest of *Nothofagus glauca*, the sclerophyll forest of *Lithraea caustica* and *Peumus boldus* and the thorny forest of *Acacia caven* and *L. caustica*, where the last two belts are defined as shrubland. Forest plantations were replaced by native forest and shrublands, reaching a total of 26.8 and 61.4% of the total catchment area, respectively.

2.5.2. Climate change scenarios

A dataset of 26 global circulation models (GCM) from the Coupled Model Intercomparison Project (CMIP5) was used to evaluate the effect

Table 3
Area of categories of land cover / uses in: present situation (CLC); present land cover with forest management (FM), future forest policy (FP); and extreme increased of forest plantations (EX); forest management (FM); forced land displacement (FLD) and pristine scenario (PR) expressed in km^2 and% with respect to the total watershed.

Scenario	Description	Pine plantations			Native shrublands			Native forest		
		km^2	%	change (%)	km^2	%	change (%)	km^2	%	change (%)
CLC	Present day land cover	266	42.9	–	264	42.7	–	17	2.7	–
FM	Forestry companies use a less intensive forest stand management	266	42.9	–	264	42.7	–	17	2.7	–
FP	Projected result of forest policy 2015–2035, where there is a partial replacement of shrubland by exotic forest plantation	327	52.7	+ 9.8	204	32.9	− 9.8	17	2.7	–
EX	Replacement of all the existing native shrublands with exotic forest plantations	530	85.6	+ 42.9	0	0	− 42.9	17	2.7	–
FLD	Exotic plantations are switched with shrubland from headwaters to lower land areas	264	42.7	−0.2	266	42.9	+0.2	17	2.7	–
PR	Replacement all the exotic forest plantations with native forest and shrublands according to potential vegetation belts	–	–	−100	381	61.4	+18.7	166	26.8	+24.1
CC-MM	Climate change from the median of 24 model projections for P and T	These climate scenarios are combined with the LULCC scenarios(CLC-CC, FM-CC, FP-CC, EX-CC, CC-FLD. CC-PR)								
CC-DH	Climate change hot and dry. Based on the mean delta of the 8 models that projected the largest change in P and T									
CC-WW	Climate change wetter and warmer. Based on the mean delta of the 8 models that projected the least warming and drying, and even a small increase in precipitation									

of future climate change. The simulations correspond to future projections following the Representative Concentration Pathway 8.5 (RCP8.5) -high emissions- scenario. We decided to use this pessimistic scenario because it seems to be the business as usual and it represents a useful tool for quantifying physical climate risk, especially over near- to midterm policy-relevant time horizon (Schwalm et al., 2020). Precipitation was first biased-corrected and interpolated to a 25x25km grid, using the methodology implemented in Bozkurt et al (2018). Monthly rainfall and the average temperature of the 26 GCMs were compared against data from the three weather stations during the period 2006–2018 with respect to the annual cycle and interannual variability. The results of the comparison indicated a good representation of the monthly climatology for all the models (Supplementary material IV), except for MIROC5 and FGOALS_g2, which were discarded of the subsequent analysis. Projected climate data were obtained using the Delta method (Quilbé et al. 2008), where future minimum and maximum temperatures are constructed by adding to the present day station data the ΔT difference from the 24 GCMs between the periods (2006–2018) and (2037–2050, see Supplementary material V). In the case of precipitation, future precipitation is obtained by multiplying present day precipitation by the *rP* change between the two time periods. The assumptions behind the Delta method include that the effect of climate change is temporarily homogeneous during each month, and the occurrence of rainfall remains the same as local data.

$$\Delta T_{(s,m)} = \frac{\sum_{2037}^{2050} T_{CC}(s,m,y)}{13} - \frac{\sum_{2006}^{2018} T_{CC}(s,m,y)}{13}$$

$$rP_{(s,m)} = \frac{\frac{\sum_{y=2037}^{2050} P_{CC}(s,m,y)}{13}}{\frac{\sum_{y=2006}^{2018} P_{CC}(s,m,y)}{13}}$$

$$T\hat{A}^{o}_{CC(s,i,m)} = T\hat{A}^{o}_{present(s,i,m)} + \Delta T_{(s,m)}$$

$$Pp_{CC(s,i,m)} = Pp_{present(s,i,m)} * rPp_{(s,m)}$$

where T = temperature, P = precipitation, s = weather station location, m = month, y = year, i = day and CC = climate change.

2.6. Evaluation of the impact of global change on water yield

To reduce the number of hydrological simulations, only three future climate change scenarios were created for each LULCC scenario: dry and hot climate change (CC-DH), climate change multi model median (CC-MM), and wetter and warmer climate change (CC-WW), representing the first, second (median) and third quartiles, respectively, of the P and T factors (ΔT, *rP* of the selected 24 CC models. CC-DH was constructed by adding to the baseline climate for each month the mean delta of the 8 models that simulated the largest change in precipitation and temperature, hence the driest and hottest case. The CC-MM was constructed by adding the multi model median for both variables, and the CC-WW by adding the 8 models with the least changes for each month, i.e., the least warming and drying, and even a small increase in precipitation. These three scenarios are used as a sort of multi-model low, median and high climate scenarios (Mishra et al., 2018), see Supplementary Material V for exact values). The relative differences of Q between the present condition (2006–2018) and different scenarios of global change were analyzed with the following equation:

$$Relative\%differences = \left(\frac{Q^{s}_{scenario} - Q^{s}_{present}}{Q^{s}_{present}}\right) * 100$$

where $Q^{s}_{scenario}$ are streamflows simulated for scenarios (LULCC and CC) and $Q^{s}_{present}$ are streamflows simulated during the present period (2006–2020). Relative percentage differences were calculated for the five LULCC scenarios, the 24 CC models, the CC-DH, CC-MM and CC-WW scenarios and the joint effect of LULCC and CC-scenarios (Fig. 1).

2.7. Spatio-temporal analysis of HRUs hydrological components

A detailed evaluation of the changes in actual evapotranspiration (ETa), Available Soil Water Content (ASWC) and Water Yield (WY) was carried out for the 206 HRUs representing Forest Plantations (98) and Shrublands (108) considering the hydrological year (April to March). Both cases were analyzed through monthly boxplots for a dry and a normal year during the megadrought. The 2016 was the driest year of the simulation period during the megadrought period (2010–2018), when annual recorded P was 464 mm and mean Q of in the Cauquenes river was 1.5 $m^3 s^{-1}$. In the absence of wet years during the simulation period, the 2015 year was considered as normal, despite being placed within the megadrought, as its annual P was 790 mm and mean annual Q of 8.1 $m^3 s^{-1}$, which were like the average hydrometeorological conditions (886 mm of P and 8.9 $m^3 s^{-1}$of Q) for the 1976–2009 period. To compute the hydrological components of HRUs during the CC period, only the CC-MM scenario was chosen. In addition, the spatial distribution of the hydrological components during these periods were also analyzed for shrubland and forest plantation HRUs, by calculation of annual means during the dry and normal years.

3. Results

3.1. Calibration and verification

We calibrated 11 parameters based on results of the Sobol sensitivity analysis. The most sensitive parameter was the curve number (CN) corresponding to tree plantations and shrublands, where the calibration range was set to 63–77 and 71–86 and, the final calibrated values were 82 and 77, respectively. The water routing parameter (CH_K) was also sensitive**.** The "best" parameter values obtained with the hydroPSO algorithm are summarized in Supplementary material III. In general, simulated Q were able to represent observed flows, except during highest winter events, when model simulations underestimate peaks greater than ~ 80 $m^3 s^{-1}$ at a daily scale (Fig. 4a and Fig. 4b).

Daily and monthly model efficiencies during calibration and validation period were similar. Nash-Sutcliffe efficiencies obtained during calibration and verification were 0.75 and 0.72 at daily time scale, and 0.88 and 0.88 at monthly scale, respectively, while the PBIAS and RSR were below 12.6% and 0.53, respectively for daily and monthly time scales (Table 4). Therefore, we consider our results as an acceptable representation of the hydrological processes occurring within our study area. In particular, a monthly time scale was considered for the further scenario analysis, since it was classified as "very good" in the calibration and verification period, in terms of NSE and PBIAS (Moriasi et al., 2007).

3.2. Climate change projections

Factors obtained through the Delta method show an increase of Tmax and Tmin for all months and all models, as well as a decrease of precipitation for most months and models, although some models and for some months project an increase in P (Fig. 5 and Supplementary material V). The construction of the three CC projections used to force the SWAT model show an average increase of 0.95 °C (CC-MM) for the period (2037–2050) with respect to (2006–2018), the CC-DH and CC-WW projections are on average 1.1 °C and 0.85 °C warmer, respectively. All three simulations (CC-MM, CC-DW and CC-WW) show largest warming in summer (DJF, 1.06 °C, 1.25° and 0.89 °C, respectively) and smallest warming in winter (JJA, 0.81 °C, 0.92 °C and 0.51 °C, respectively). Tmin are also projected to increase during all months and all models, but in a smaller amount. In the annual mean the CC-MM, CC-DH and CC-WW simulations increase 0.79 °C, 0.94 °C and 0.62 °C, respectively. Again, smallest increases are found for winter (0.61 °C, 0.72 °C and 0.47 °C, respectively), and largest for summer or autumn. For precipitation, in the CC-MM scenario the average monthly Delta factor is of 0.91, which represents a decrease in P in the order of 9%. The largest

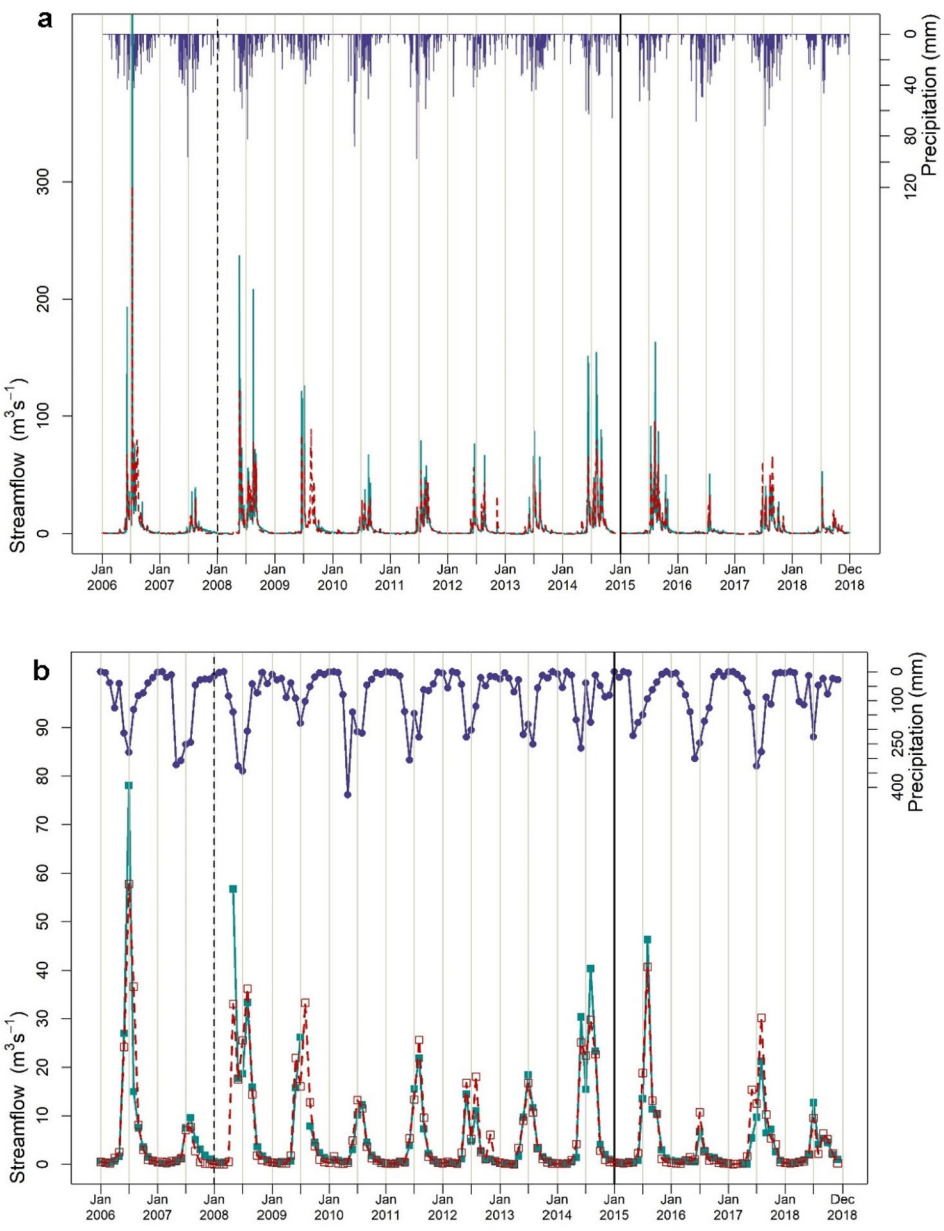

Fig. 4. Flow simulations ($m^3 s^{-1}$) (a): daily and (b): monthly scale. The calibration period is shown to the left of the vertical black line and the validation period to the right. The simulated data is shown with red dotted line with empty red squares and the observed data is shown in green solid line with solid squares. Mean observed Precipitation (mm) from the three DGA meteorological stations is shown at the top of the graph. (For interpretation of the references to colour in this figure legend, the reader is referred to the web version of this article.)

Table 4
Performance indices of the SWAT model simulations compared to the observed flow data. Calibration considered the 2008–2014 period, and verification the 2015–2018 period. The NSE, RSR and Pbias (%) are shown daily and monthly for the calibration and validation periods.

	Calibration		Verification	
	Daily	Monthly	Daily	Monthly
NSE	0.75	0.88	0.72	0.88
RSR	0.5	0.36	0.53	0.34
Bias (%)	2.8	−2	12.4	12.6
KGE	0.78	0.86	0.81	0.85

NSE is the Nash-Sutcliffe goodness-of-fit index, RSR is the relationship between the mean square error and the standard deviation of the data, and Bias (%) is the percentage of bias.

decreases are projected for summer (DJF, 14%) and smallest in autumn, of only 1%. Only six models showed delta values larger than 1 for P, depicting an increment in the annual mean (e.g., CSIRO_Mk3_6_0 with an average delta of 1.6). However, most of the models (i.e., 18) showed delta values lower than 1 for P, with the lowest value of 0.66 for the IPSL_CM5A_LR. The scenarios CC-DH and CC-WW correspond to annual mean P changes of 19% decrease and 4% increase, respectively. Note that although the CC-WW corresponds to a scenario with an overall increase of P, summer and spring do not show a change and autumn and winter show a 4% and 5% increase with respect to (2006–2018), respectively.

3.3. Flow impact assessment

For the current climate period (2006–2018), Fig. 6a and Supplementary material VI) show the relative differences of mean annual Q between present Land cover and the LULCC scenarios. A decrease of 2.5 and 17.3% of mean annual Q is observed for the FP and EX scenarios, and the decrease is accentuated in June, with a median decrease of 4.5 and 31.8%, respectively. Practically no changes in Q were detected for the FM adaptive management scenario. The FLD scenario showed a general increase in flow with a mean annual increase of 2.3%, and mean monthly values ranging from −0.1% in September to 4.1% in April. The

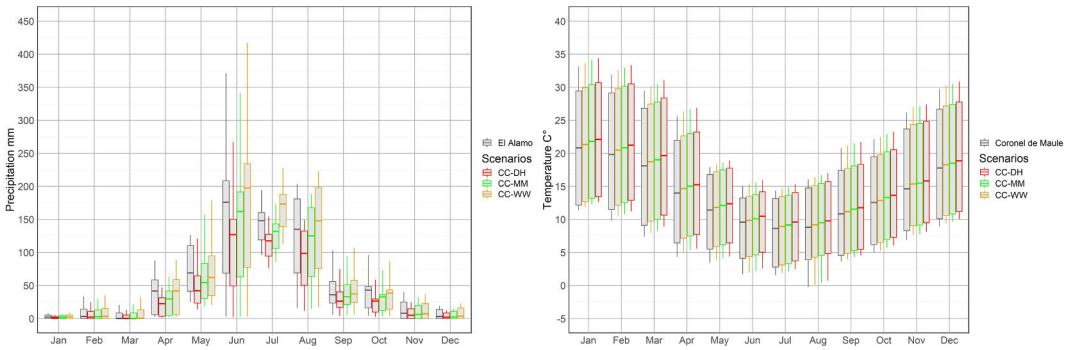

Fig. 5. Monthly values of precipitation and temperature for the dry and hot climate change (CC-DH), climate change multi-model median (CC-MM) and the wetter and warmer climate change (CC-WW) scenarios for the period 2037–2050 and present precipitation and temperature data (2006–2018) in the El Alamo and the Coronel de Maule weather stations, respectively.

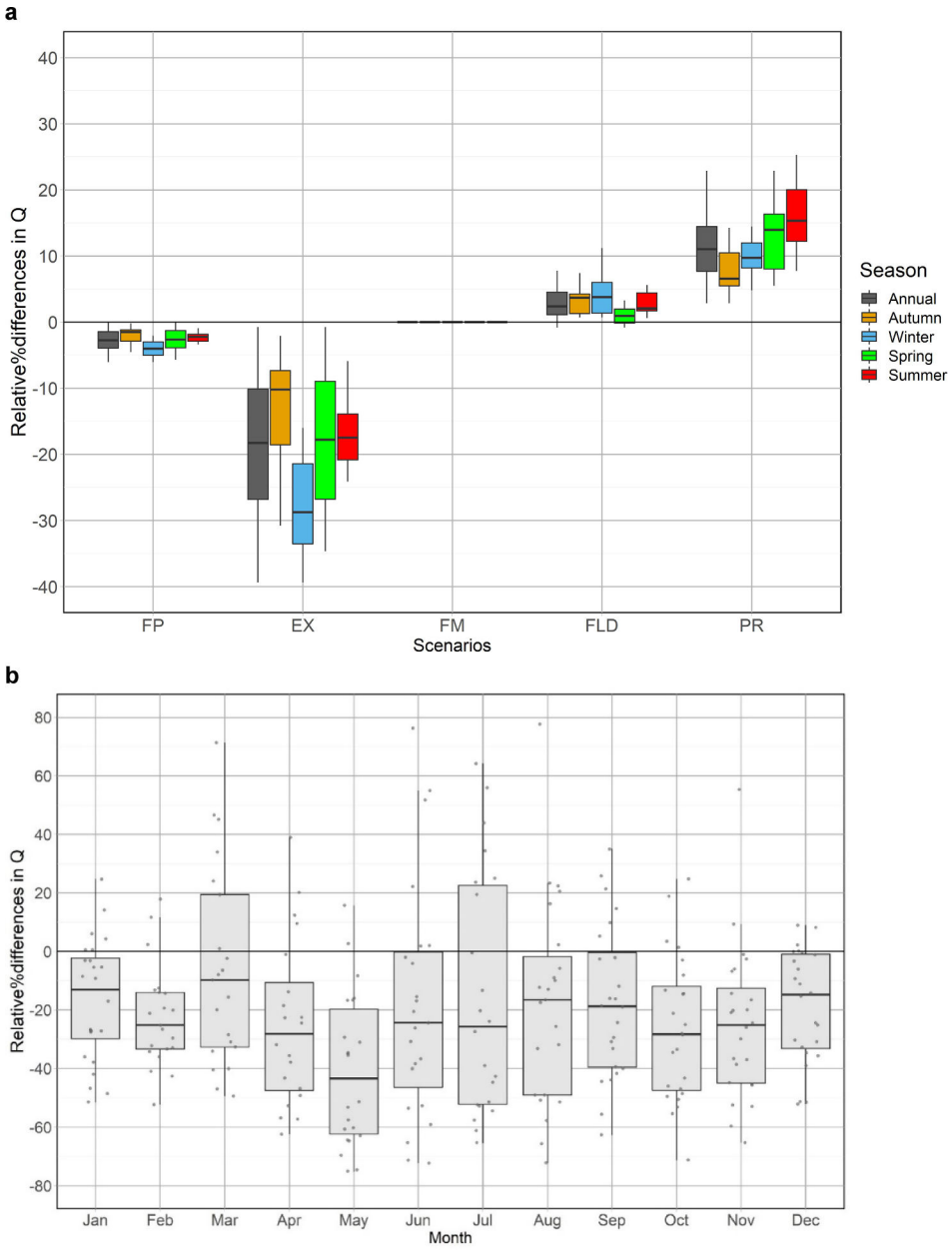

Fig. 6. (a): Relative percentage changes in streamflow rate with scenarios of land use change / coverage at yearly and seasonal. (b): Relative monthly percentage differences in streamflows between the present condition (2006–2018) and the future condition forced by the 24 RCP8.5 climate Change models (2037–2050).

largest increase was observed for the PR scenario, with a 10.9% increase in mean annual Q, with positive values in all months, the lowest increase in April (3.9%) and highest increase in December (15.2%).

Hydrological simulations driven by the 24 climate change models and by the three future climate change scenarios (CC-DH, CC-MM, CC-WW) with the current land cover are displayed in the CLC-CC scenario of Fig. 6b and Fig. 7, respectively. A general reduction of Q is observed when analyzing the 24 CC models individually, according to monthly median reductions ranging from 17.1% in March to 57.4% in May. However, large spread in Q simulations is also observed according to the size of the monthly boxplots which ranges up to 100% in July, depicting positive values of relative difference in Q for all months. In CC-MM a general decrease of 32% is found for Q, with largest decreases simulated for autumn (MAM) of about 35% and lowest in summer (DJF) of 27%. In CC-DH a sharp decrease of 61.5% is found, with largest decreases simulated for winter (JJA) of about 63% and lowest in summer of 58%. In CC-WW an increase of 9% is found, with largest increases simulated for winter (JJA) of about 20% and decreases in spring of 1%.

The combined effects of LULCC and CC scenarios on Q are displayed in Fig. 7. When calculating streamflow differences with the CC-MM, Q decreases, regardless of the land use scenario used. Effects are largest for the EX simulation with a decrease of 46.6%, followed by the FP and current land cover scenario (CLC) with decrease of 34 and 32%, respectively. Adaptive management scenarios showed Q decreases of 31.7, 29.5 and 22.3% for FM, FLD and PR scenarios, respectively (Supplementary material VI). When analyzing the effect of LULCC under CC-DH scenario on Q, a similar hierarchy of Q decrease was found, with a sharp decrease for EX, FP and CLC, with values of 72, 63 and 62%, respectively. Adaptive scenarios showed a lower decrease on Q with values of 62, 60 and 56% for the FM, FLD and PR scenarios, respectively. The CC-WW scenario depicted a decrease on Q only for EX with a value of 8%. Increases on Q were found for the rest of LULCC scenarios with values of 9, 7, 9, 12 and 24%, for CLC, FP, FM, FLD and PR, respectively. Increases on flow are consequent with the projected precipitations which on average increases about 8% with respect to the P over the 2006–2018 period. Seasonal trends of Q are similar than annual trends, however summer Q showed lower decreases than the rest of the seasons for the CC-MM and the CC-DH scenarios. This is especially visible for PR, with decreases on Q of 50 to 14% for CC-DH and CC-MM. Winters Q also followed a different trend for the CC-WW scenario, with larger increases for the CLC, FP, FM and FLD with respect to other seasons (Fig. 7).

3.4. 3.4 Impacts on hydrological processes

Fig. 8 shows boxplots with the monthly values of actual evapotranspiration (ETa) for the HRUs (Fig. 8a, b), Available Soil Water Content (ASWC) (Fig. 8c, d), and Water Yield (WY) (Fig. 8e, f), of exotic forest plantations (FRSE) and native shrublands (SHRB), for a normal and dry year both under present (-P), and projected climate conditions (–CC). For the normal year under the present climate conditions, ETa (Fig. 8a) showed a marked seasonal dynamic, especially for *P. radiata*, (FRSE) with an increasing trend from August to December, where the maximum values are reached. Then, a sharp decrease in ETa throughout the summer months (DJF) until reaching the lowest levels in February. Shrublands (SHRB) showed a lower ETa dynamic, with similar seasonality throughout the year, and the maximum values reached in October. They present lower amounts of ASWC (Fig. 8c) than exotic plantations during winter. However, a sharp decrease starts in October for exotic plantations and extends until completely deplete it in January, while shrublands keep ASWC during the whole year. Regarding water yield (WY) (Fig. 8e), it showed a visible seasonality for the two land covers, with high values in winter and practically zero values in summer for both land covers. A large spread is also observed in July and August (winter), with higher variability for shrublands.

In comparison to the normal year, the dry one present a similar seasonality and magnitude of ETa and ASWC for shrublands, which is not the case for *P. radiata* where an important reduction and an earlier decrease are observed (Fig. 8b, d). Total yearly ETa was reduced from 709 to 623 mm for exotic plantations. Extremely low values of WY are observed for both land cover all along the year, especially for exotic plantations (Fig. 8f). The latter situation agrees with the precipitation (464 mm) and streamflow (1.5 $m^3 s^{-1}$) levels of this year (2016).

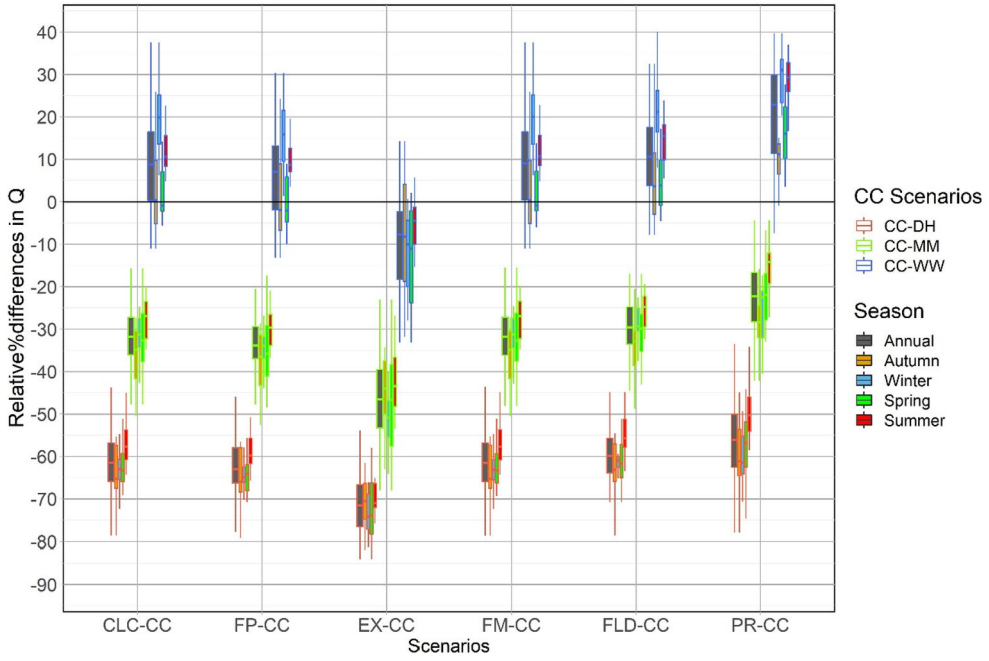

Fig. 7. Relative percentage changes in streamflow with combined effect of land use change/ cover and climate change scenarios (CC-DH, CC-MM and CC-WW) at yearly and seasonal scale. CLC-MM: is current land cover represented with the climate change Multi Model Median (CC-MM); FP: Forestry Policy; EX: Extreme scenario; FM: Present Land cover with forest management; FLD: Forced Land Displacement; and PR; Pristine Scenario.

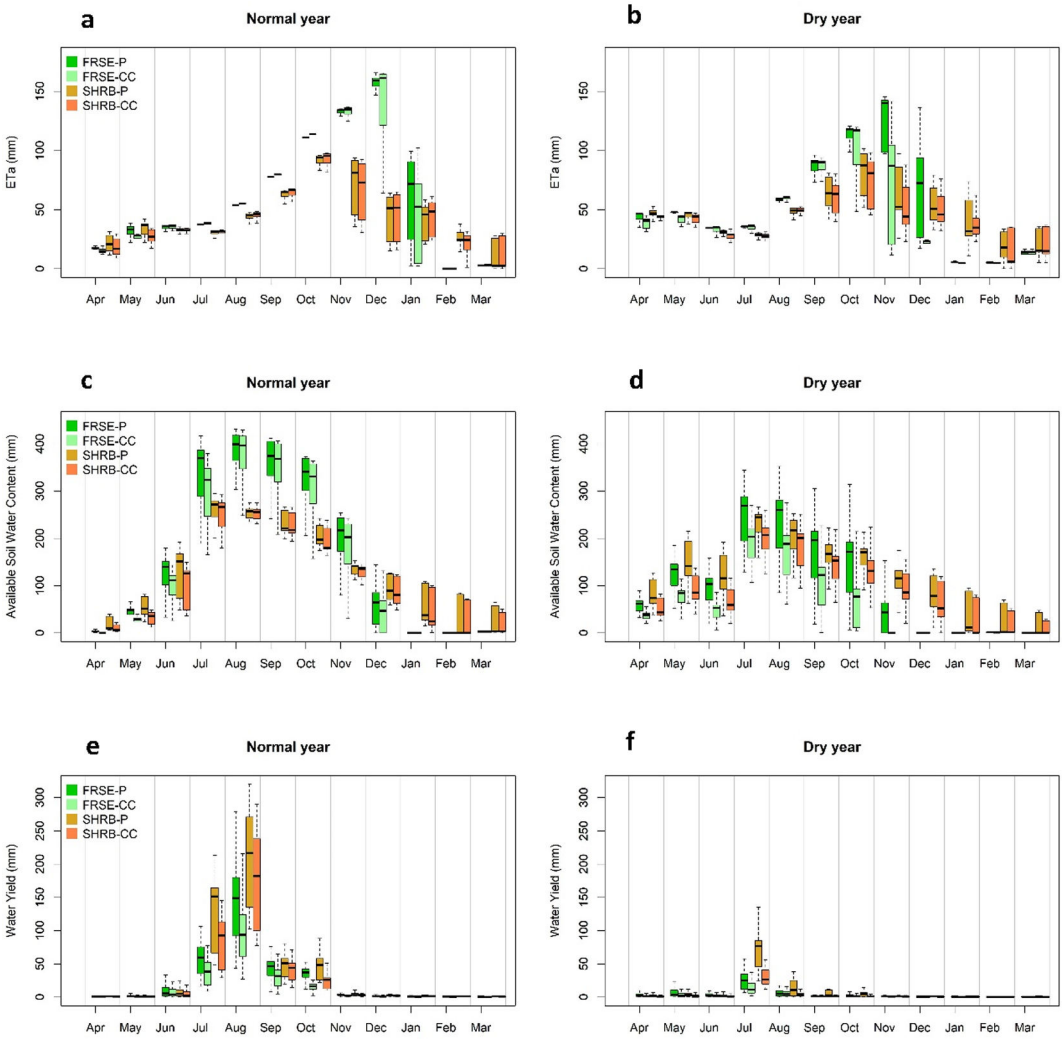

Fig. 8. Boxplots of the Pine plantation (FRSE) and Shrubland (SHRB) HRUs for a normal year and a dry year for the variables: (a) ETR (mm), (b) Soil Water (mm) and (c) Water Yield (mm) plotted for the present situation and with climate change represented by CC-MM.

Considering the projected CC scenarios in a normal year, a similar seasonality and magnitude is observed for ETa and ASWC for both land covers in comparison to the present climate (Fig. 8a, and Fig. 8c). This was not the case for WY where an important decrease is projected. Under drier future projections, a reduction of ETa and ASWC is estimated for both land covers, especially for *P. radiata*, where yearly ETa diminished from 683 to 518 mm (Fig. 8b, c). Earlier decrease is also estimated with ASWC depletion in November. Finally, Fig. 8e shows a sharp decrease in WY for both land covers in winter (JJA) months, where the total yearly WY did not exceed 32 mm for pines.

The present spatial distribution of hydrological components is displayed in Fig. 9, for a normal and dry year, respectively. A clear spatial relation between precipitation and ETa is depicted, with high values located at the high-elevation lands in the western part of the catchment (Fig. 2). This relation was consistent during normal and dry years. The eastern part of the catchment, where abundant forest plantations are present (Fig. 3), exhibited relatively high values of ETa ranging from 605 to 658 mm of ETa under normal years (Fig. 9b), however this situation changed for the dry year where the same area showed much lower values, ranging from 446 to 507 mm of ETa (Fig. 9e). WY showed a different spatial pattern, with high values in normal years located in the high-elevation areas of the northwestern and central part of the catchment (Fig. 9**c**). Lower values of WY are observed for the western and southeastern part of the catchment, where most of the exotic forest plantations are located (Fig. 9c and Fig. 3). During the dry year, WY a considerable reduction in WY magnitudes was observed (e.g., maximum range fall from 717 mm to 214 mm). The western area, mainly cover with exotic plantations, showed a marked decreased in WY, moving from 300 to 400 mm in normal year to 50–100 mm in a dry year. (Fig. 9f and Fig. 3).

4. Discussion

4.1. Impact of LULCC

The decrease in Q observed with the expansion of exotic forest plantations (FP and EX scenarios) is in agreement with different reviews and *meta*-analysis documenting that afforestation with non-native species have reduced water yield in different regions of the world, and that this decrease is enhanced under dry conditions (e.g. Farley et al., 2005; Scott & Prinsloo, 2008; Filoso et al., 2017; Zhang et al., 2017; Ferraz et al., 2019).

Several studies report the negative effect of the expansion of forest plantations on streamflow in Mediterranean areas. In an Australian catchment with an ET/PP ratio similar to our study, the conversion and replacement of 10 to 50% of the pasture area with plantations, generated a decrease in Q between 1 and 3.6% (Nguyen et al., 2017). This is like the 2.5% decrease in Q reported in our catchment, when 10% of the area originally covered with shrublands is replaced by plantations, but less than the −17.3% change in Q, when 43% of its area covered with

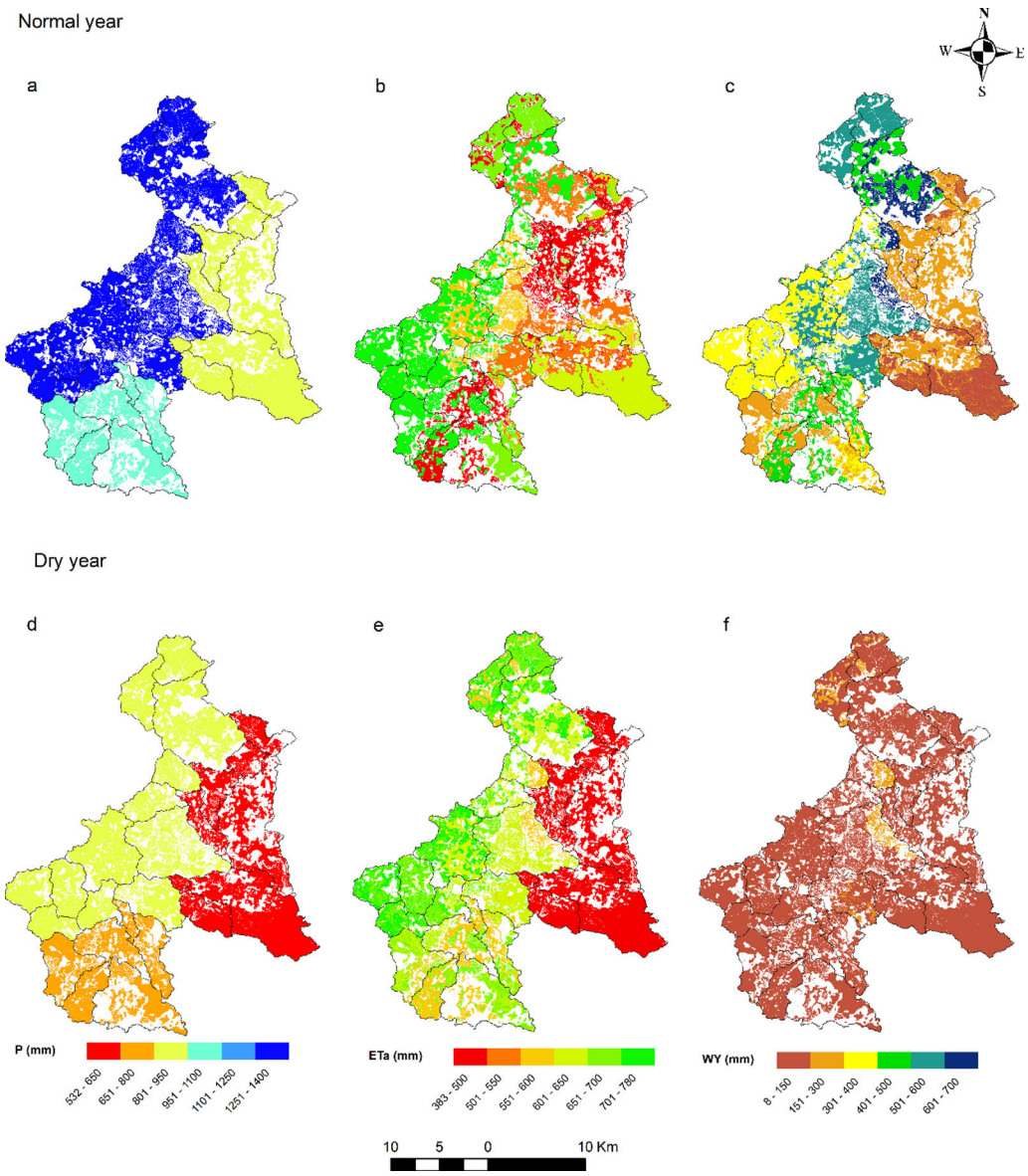

Fig. 9. Spatial representation of yearly values of Precipitations (P) Actual Evapotranspiration (ETa) and Water Yield (WY) in mm yr^{-1} for HRUs. Panels a, b and c, represent a normal year (2015) according to average hydrometeorological conditions of P and Q. Panels d, e and f, the represent the dry year 2016 which is one of the driest year of the current Mega-Drought period according to its P and Q.

shrubland is replaced by pines. These differences could be explained by the size of the catchments, since Cauquenes is three times bigger than the one studied by Nguyen et al., (2017), and this could amplify the Q decrease in our study (Pilgrim et al., 1982; Gallo et al., 2015). In spite of these differences, similar results have been reported by Carvalho-Santos, et al., (2016) in a Mediterranean catchment in Europe, with a decrease of 7% when introducing 63.5% of eucalyptus plantation.

In the southern portion of the temperate Mediterranean region of Chile (38°-39° S), with a mean annual precipitation of 1650 mm, and a dry season of five months, Stehr et al., (2010) reported a reduction of 10.6% in Q for a scenario of 96% increase in exotic forest plantations for the Vergara catchment (133 km^2) at the expense of shrublands and agricultural lands. Their estimate is lower compared to the 17.3% estimated in Q for our EX scenario with a 43% increase in forest plantations area. Higher precipitation and a different soil pedogenesis; with deeper volcanic soils, in contrast to the Lithosols present in Cauquenes, which are shallower and with a higher bulk density and lower water storage capacity (Soto et al., 2019), may explain differences in the magnitude of streamflow reduction. Alvarez-Garreton et al. (2019) carried out a regression model in 25 Chilean catchments to assess the impact on Q from the replacement of several land cover classes with exotic tree plantations. Their study considered Cauquenes catchment as one of the 13 drier catchments (aridity indices ranging from 0.17 to 1.5, and they found a 3%decrease in Q after a replacement of 6000 ha of shrublands in this catchment. These results were like the change obtained for our FP scenario (-2.5%) in which 5600 ha of shrublands were replaced by *P. radiata*. The consistency of the decrease in Q obtained by this statistical approach and our process-based modelling results reinforce the confidence in the robustness of our analysis. Another study done at the Cauquenes catchment, documented forest plantation area increased from 20 to 42% (22%) from 1990 to 2000 and estimated a 31.9% reduction in summer streamflow for the period 1991–2000 compared to 1981–1990 using a linear model from the changes in runoff (Q/P) residuals (Little et al., 2009). Their estimate is higher than the 17.3% decrease in Q for our EX scenario, where forest plantations increased by 43%. Despite using different methods and reference periods, differences between both estimates might be explained by the steep reduction of streamflow during the first rotation of plantations when they were not

only expanding but actively growing with similar age classes before the first clear-cut. Conversely, the model built in this study estimated the water yield of plantations compared to other land uses for the 2006–2018 period, when plantations formed a mosaic of age classes and development stages after two or three 16–18 year rotations that are commonly used for pines in Chile. This becomes clear since total area of plantations was estimated in 42% for 2000 (Little et al., 2009), which remains stable (43% in 2016 estimated by us), indicating this shifting mosaic of age classes that buffers the effect of plantations on reducing streamflow, as they age in short rotations (Farley et al., 2005). This indicates that streamflow for the FP and especially for the EX scenario might probably reach a much lower value when all the plantations are in their first rotation in the next 15–20 years (i.e. in 2033–2038) than the one we estimated for the 2037–2050 period.

Adaptive scenarios (FM, FLD, PR) showed positive to neutral responses, highlighting the role of native vegetation and possible restoration strategies. The less intense stand plantation management scenario (FM in Fig. 6a), represented with a decrease in maximum LAI, did not produce important changes in Q. This was a counterintuitive result given the evidence about the importance of this variable in the use of water in tree plantations (Barrientos & Iroumé, 2018). The sensitivity of this parameter in the SWAT model seems to be misrepresented under certain forest ecosystems (Yang and Zhang, 2016). Nonetheless, the FLD scenario showed an increase (+2.3%) in Q, resulting in a partial mitigation of the impact of tree plantations. Results regarding the strategy proposed in our FLD scenario highlights that protection of headwaters with native ecosystem seems to be able to favor infiltration and hence water availability downstream (Buttle, 2011).

The pristine (PR) scenario showed an 11% increase in annual Q for a change in native area cover from 2.7% in 2018 to 26.8% (24.1% increase). This increase is like the 14.1% rise in summer streamflow for each 10% increase in native forest area estimated for the temperate region of Chile (40° S, 1700–2500 mm annual precipitation, Lara et al 2009). It is interesting the similarity between both estimates despite their different methodology in which Lara et al. (2009) used a linear model that considered six 55–1460 ha catchments, and native forests covered between 20 and 90% of each catchment with the reminder represented by forest plantations and shrublands (Lara et al., 2009). The increase in Q from the restoration of native forests documented for the PR scenario might revealing a likely better ecosystem response to disturbances such as the current megadrought and its consequences. For example, the 2017 mega-fire, that affected the region (Bowman et al., 2019), could have been less severe under improved soil conditions and water content (e.g. Soto et al., 2019) that might be enhanced by the restoration of native forests. Given these positive results on Q, it would be of interest to analysis them also in the context of other benefits related to the UN Sustainable Development Goals (SDGs, UN, 2015), like reduction of poverty (SDG1), access to clean water (SDG 6) and Life on Land (SDG15) for example.

4.2. Impact of climate change

During the period 2010–2018 precipitation and streamflow have decreased a 33% and 46%, respectively, in comparison to the period 1976–2009. The climate change scenarios used in this study, project a further precipitation and streamflow decrease of around 15% and 32% respectively, as well as a 0.95 °C of warming. From the relative differences in Q, it can be inferred that climate change is the greatest driver of the decrease in Q (Fig. 7). The reduction in P and the increase in atmospheric demand triggered by higher air temperatures are the main drivers that explain those trends in Mediterranean catchments (Brown et al., 2015; Molina-Navarro et al., 2016). Regarding the magnitudes of change obtained in this study (–32% at yearly scale, ranging from + 9 to −63% for the CC-WW and CC-DH simulations, respectively), similar results have been reported with simulations carried out with the Variable Infiltration Capacity (VIC) hydrological model for the Maule catchment (which contains the Cauquenes catchment), which projected an annual runoff decrease of approximately 20%, ranging from 5% increase to 60% decrease for the medium term (2040–2069) and under the RCP8.5 scenario (Bozkurt et al., 2018). The pluvial nature of the Cauquenes catchment could explain the sharp decrease on median flows (–32.1%) (Fig. 7) as compared to Maule catchment, which has more nival contribution (Fig. 2). A sharper decrease of Qs would be obtained (not shown), if a longer historical climate period (1979–2006) would be chosen instead of the current one (2006–2018). This later period includes the mega-drought, which as mentioned above has already seen a 46% decrease in Q with respect to the historical period. Hence, the climate change effect must be considered with caution since it already includes the current mega-drought effects.

4.3. Impact of the combined effect of CC and LULCC

The combined effect of CC and LULCC have strong synergies, with decreases in Q ranging from 22 to 47%. These results depict a much stronger reduction in Q than previous studies in Mediterranean catchments of Europe. For example, a study of two catchments in Portugal showed Q reduction ranging from 13 to 18% (Serpa et al., 2015). In these catchments, the decrease in Q was largely dominated by the CC effect, and the drier catchment present a larger decrease of Q. Another study from the Vez catchment also in Portugal under more humid climate, showed a reduction of 9% annual water yield (Carvalho-Santos et al., 2016), while the effect of CC only reduced water yield from 1 to 2%, being larger the effect of afforestation with exotic plantations. In this study the CC effect is greater than the one from afforestation, which could be explained by the more severe RCP scenario chosen (8.5 instead of 4.5) and more severe projections of precipitation reductions for central Chile than for south western Europe (Collins et al., 2013; IPCC, 2013). In the European catchments, a sharp decrease of summer Q was reported, which is not case in our study for FP and EX scenarios. A possible explanation is related to differences in the history of land use changes. In Cauquenes large afforestation has already happened in the past (Little et al., 2009) and currently 43% of the area is covered with exotic forest plantations, meanwhile in the Vez European catchment, native shrublands and forests dominate the area. This idea is reinforced when analyzing the adaptive scenarios, since in both, summer Q are increased for CC projections (Fig. 7).

The Pristine (PR) scenario allowed an important mitigation of the impact of CC on Q reduction, even with streamflow increases for the CC-WW simulations. This highlights the importance of preserving and restoring native forests for the recovery of water provision as a key ecosystem service, stressing the need to consider both actions in the National Strategy for the Adaptation to CC in Chile (Little and Lara, 2010; Lara et al., 2013). The increase in Q observed during summer for the FLD and PR scenarios are especially important, since they represent the only possible source for drinking water and irrigated agriculture, therefore, strengthening the relationship between local water and food security. These human primary necessities can be crucial in this territory, affected by a structural poverty condition (Pino et al., 2015). The positive impact of these LULCC scenarios should be evaluated under their broader co-benefit and synergies to fulfill several SDGs.

4.4. Impacts on hydrological processes

Yearly simulated ETa values during the present climate (626 to 751 mm) for *P. radiata* were in agreement with those found in southern Australia, where transpiration values ranging from 500 to 612 mm were obtained with two different formulations of a process-based ecosystem model (Sheriff et al., 1996). Other studies in Chile estimated values of 545 to 654 mm of yearly ETa, using a residual water balance approach, in an area with slightly higher rainfall (between 846 and 1056 mm, including areas with clay-rich soils) (Huber and Trecaman, 2004). With respect to direct measurements of ETa using Eddy covariance systems,

values between 399 and 488 mm were registered in New Zealand for a young 8-year-old plantation established at high density (Arneth et al., 1998), consequently higher amounts are expected for mature pines. Similarly, Putuhena & Cordery (2000) evaluated components of the water balance in *P. radiata* plantations, obtaining an annual ET/Pp ratio of 68% on average, being similar to the 65% obtained in our study area. These results allow us to accept our yearly simulations of ETa for *P. radiata* as reasonable enough to draw conclusions about the effect of land cover replacement on Qs. Simulated ETa on shrublands was like those reported by Meza et al., (2018), for which, ETa/P ratio of 0.64 was measured by an eddy covariance system in a much drier area of central Chile (200 mm of annual precipitation). Discrepancies in terms of ETa magnitudes (506 mm in Cauquenes compared to 128–139 mm in the study of Meza et al. (2018), could be explained by the larger water stress condition of shrublands reported in the study of Meza et al. (2018). In this sense, shrublands in our study area are taller, with higher density and vigor, and with more pastures in the surroundings, which suggests that their water consumption should be greater. In addition, the shrubland composition often includes species of mid to late successional stage of the sclerophyll forest such as *Lithraea caustica* (Luebert and Pliscoff, 2018), which has higher water requirements than the *A. caven* shrubland (Bown et al., 2018).

Hydrological components for the two land cover classes analyzed in this study allow us to conclude that there is a distinctive response in water yield during drier or wetter years. Our results showed that WY is much lower during the dry year than during the normal year, especially for HRUs with *P. radiata*, explained by the reduction in ASWC (Fig. 8d) while keeping high rates of ETa (Fig. 8b). Despite this situation, our results showed a 12% decrease in ETa for *P. radiata* under drier conditions, which was exacerbated in our CC scenarios, with larger decreases (27%) compared with a normal year without CC. The consequences could not only affect local water yield and Q, but also forest plantations growth (Alvarez et al., 2012; Navarro-Cerrillo et al., 2018), thereby increasing susceptibility to wildfires (Bowman et al., 2019), diseases caused by insects Anderegg et al. (2015), and especially water stress for young pine plantations (which are especially susceptible due to their undeveloped rooting systems) (Yang et al., 2018). These effects indicate a low ecological resilience of *P. radiata* plantations to drier conditions, which has been reported for other planted pine species of Spain (Guada et al., 2016). This could threat the sustainability of the current forestry model and the international commitments towards carbon neutrality (NDC). In contrast, our simulations suggested a better ecological response of shrublands during dry periods, because they maintained a low ETa rate, preserving ASWC and hence more water yield at the HRU scale. This eco-hydrological behavior was measured for *Acacia caven* shrubs, where the soil water beyond 100 cm deep was not used, leaving the remaining water for the following year as a reservoir (Sepulveda et al., 2018). Policy strategies based on massive afforestation to mitigate the impacts of climate change on water resources should be revised, considering that in a drier future, carbon allocation would not be granted by exotic forest plantations, which can suffer from severe productivity restrictions in Mediterranean-like catchments. Of particular interest was the shrublands response, which seems able to better manage reductions in water availability, as demonstrated by the similar ETa rates during both dry and normal years, which could be an indication of a stable carbon sequestration.

The spatial distribution of hydrological components in normal and dry years depicts an expected pattern for P and ET, with higher levels in elevated areas where more water as P is available (Fig. 9b). Similar spatial patterns for ETa under normal years was previously reported for the same study area (Olivera-Guerra et al., 2014), derived from a surface energy balance model based on satellite observations, reinforcing the confidence in the results of our simulations. Of particular interest is the low ETa rate reported in the lowland eastern zone, dominated by forest plantations during dry years, probably an indication of water stress. The low levels of water yield and available soil water content (data not shown) in the same area confirm a possible situation of growth limitation, affecting carbon sequestration and productivity (Ojeda et al., 2018). Another interesting result is the substantial change in WY magnitudes in the headwaters covered with pine plantations when comparing the normal and dry years. This area maintained their ETa but considerably reduced WY. This could have consequences since this WY is critical to provide drinking water to downstream population and to sustain subsistence farming, which is common in this area due to local poverty levels (Pino et al., 2015). Some remnants of one of the most diverse forest ecosystems of the Chilean Mediterranean *hotspot* with a high degree of endemism (Mittermeier et al., 2004) are also located in this area. Therefore reduced water yield could seriously push it to the risk of collapse, according to its endangered present situation (Alaniz et al., 2016). This condition will be stressed under CC according to our simulations (data not shown), highlighting the current and future vulnerability of the territory. The FLD scenario was built to alleviate this situation, however only a slight increase in Q was observed in this scenario. Conversely, in the PR scenario an important increase in Q was observed, suggesting that more substantial actions regarding protection and restoration of native forests should be taken to cope with water scarcity under climate change (Lara et al., 2013).

4.5. Simulation limitations

Estimation of water use by the different vegetation types when the default SWAT parameterizations are used for our study area, could lead to unrealistic representation of the carbon fluxes pathways (eg. radiation use efficiency), especially nonagricultural land covers classes (Yang and Zhang, 2016). Another issue is the real capability of water extraction by the roots of forest species, since *P. radiata* and *A. caven* species are capable of extracting water from the soil below the conventional permanent wilting point thresholds (Huber et al., 2010; Meza et al., 2018). In this sense, forest covers also can extract water from the coarse fraction of soil which is not considered in the SWAT parameterization (Algayer et al., 2020). Those issues could lead to an underestimation of the real capability of water extraction by the roots affecting ETa estimations, especially during dry periods. Therefore, simulations regarding ETa dynamics should be taken with caution, even if reasonable yearly values were obtained. Another limitation frequent in Q simulations at the catchment scale is the amount and quality of soil information. In our case this could remain highly uncertain, even introducing local measurements of soil depth, given large differences in soil physical properties according to land use (Soto et al., 2019). Finally, spatial variation of P, especially with elevation, could affect the daily and monthly water balances. Even if we used a grid of P correctly validated by our local rain gauges, heavy rainfall events can occur at high elevations, as the episode of July 2019, where more than 150 mm d^{-1} (exceptionally high) were recorded at the headwaters. This is not represented by the P grid used in this study and could lead to underestimation of Q, especially at daily scale.

Adequate simulations of Q under CC scenarios largely depend on the availability of local CC models. In our study we used a simple but robust approach to represent the future climate conditions at the regional scale, however, more sophisticated methods do exists to cope with temporal variability of projections (Bozkurt et al., 2018; Piani et al., 2010). Finally, another important issue not addressed in this study is the potential effect of increased atmospheric CO_2 concentrations on water use efficiency that could buffer the effect of a dyer climate on forests and other vegetation (Swann et al., 2016), therefore affecting all components of the water balance.

5. Conclusions

The study confirms a general decrease of water availability under global change scenarios, which include five LULCC scenarios and climate change projections, for a rainfed Mediterranean catchment mainly covered with exotic industrial plantations of *Pinus radiata* and

native shrublands mainly covered by *Acacia caven*.

LULCC scenarios related to the replacement of shrublands by pine forest plantations under present climate, showed a decrease of annual Q of 2.5 and 17.3% for the scenarios Forest Policy 2015–2035 (FP) and extreme (EX), respectively. Adaptive scenarios showed a positive to neutral response, highlighting the role of native vegetation and the need of including them in future restoration strategies. The Forced Land Displacement (FLD) scenario, where plantation located in headwaters were moved downstream within an ecological restoration scheme, resulted in an average increase of Q of 2.3%, while in the Pristine scenario we got and estimated increase of 10.9%. The latter highlights that protection of headwaters with native ecosystems seems to be able to favor infiltration and hence water availability downstream.

Climate change alone leads to a reduction in P of 15% and in increase in air temperature of 0.95 °C in our study area, directly affecting potential ET. This situation amplifies the effect on Q, with a sharp decrease of 32.1% in annual values with respect to current climate (2006–2018). Although, when considering all 24 CC future projections, variations in future Q could be positive (10% increase for low warming and winter and spring precipitation increases). The latter is with respect to a base period that includes the mega-drought period, where Q has already decreased over 40% in the study region, which provides a strong support for expecting drier future condition with respect to the historical period in this Mediterranean region.

The combined effect of CC and LULCC leads to a negative synergy, with decrease in mean annual Q ranging from 46.2% (EX), to 23.3% (PR). Adaptive scenarios partially reduce the negative effect of CC in streamflows, especially during summer months when no other water resources are available, strengthening the relationship between local food and water security. This finding highlights the importance of preserving and restoring natural vegetation to alleviate the negative impacts of CC on water resources.

We found a low resilience of forest plantations to drier conditions in comparison to native shrublands, as shown by an earlier depletion of soil water content and a reduction in actual ET. The tradeoff between the water and carbon cycle imposes limitations to carbon sequestration, therefore compromising the Chilean carbon policy adopted to cope with climate change. A redesign of current and future land management strategies and the implementation of ecological restoration at catchment scale is urgently required to cope with the decrease in water availability imposed by climate change in south-central Chile. Decisions on future land management should include co-benefits analysis to fulfill several Sustainable Development Goals at the same time.

We expect the results presented in this study might have clear policy implication for Chile and other countries where the allocation of state subsidies for the expansion of exotic plantations competes against the conservation and restoration of native vegetation. The streamflow impacts of different land covers classes should be an important component of the discussions in this regard.

CRediT authorship contribution statement

Mauricio Galleguillos: Conceptualization, Methodology, Investigation, Writing - original draft, Supervision, Project administration, Funding acquisition. **Fernando Gimeno:** Formal analysis, Investigation, Software, Validation, Visualization. **Cristóbal Puelma:** Conceptualization, Methodology, Formal analysis, Data curation. **Mauricio Zambrano-Bigiarini:** Writing - review & editing, Conceptualization, Methodology, Software. **Antonio Lara:** Conceptualization, Supervision, Writing - review & editing. **Maisa Rojas:** Supervision, Data curation, Writing - review & editing.

Declaration of Competing Interest

The authors declare that they have no known competing financial interests or personal relationships that could have appeared to influence the work reported in this paper.

Acknowledgements

This research was funded by FONDECYT regular grant no. 1171560 and by the Center for Climate and Resilience Research (CR2, CONICYT/FONDAP/15110009). This work is also a contribution to the TanDEM-X DEM_GEOL0845 project.

Appendix A. Supplementary data

Supplementary data to this article can be found online at https://doi.org/10.1016/j.jhydrol.2021.126047.

References

Alaniz, A.J., Galleguillos, M., Perez-Quezada, J.F., 2016. Assessment of quality of input data used to classify ecosystems according to the IUCN Red List methodology: The case of the central Chile hotspot. Biol. Conserv. 204, 378–385. https://doi.org/10.1016/j.biocon.2016.10.038.

Algayer, B., Lagacherie, P., Lemaire, J., 2020. Adapting the available water capacity indicator to forest soils: An example from the Haut-Languedoc (France). Geoderma 357. https://doi.org/10.1016/j.geoderma.2019.113962.

Álvarez, J., Allen, H.L., Albaugh, T.J., Stape, J.L., Bullock, B.P., Song, C., 2012. Factors influencing the growth of radiata pine plantations in Chile. Forestry 86 (1), 13–26. https://doi.org/10.1093/forestry/cps072.

Alvarez, E., Duque, A., Saldarriaga, J., Cabrera, K., de las Salas, G., del Valle, I., et al., 2012. Tree above-ground biomass allometries for carbon stocks estimation in the natural forests of Colombia. For. Ecol. Manage. 267, 297–308. https://doi.org/10.1016/j.foreco.2011.12.013.

Alvarez-Garreton, C., Lara, A., Boisier, J.P., Galleguillos, M., 2019. The impacts of native forests and forest plantation on water supply in Chile. Forests 10 (6), 473. https://doi.org/10.3390/f10060473.

Alvarez-Garreton, C., Mendoza, P.A., Pablo Boisier, J., Addor, N., Galleguillos, M., Zambrano-Bigiarini, M., Ayala, A., 2018. The CAMELS-CL dataset: Catchment attributes and meteorology for large sample studies-Chile dataset. Hydrol. Earth Syst. Sci. 22 (11), 5817–5846. https://doi.org/10.5194/hess-22-5817-2018.

Anderegg, W.R.L., Hicke, J.A., Fisher, R.A., Allen, C.D., Aukema, J., Bentz, B., Zeppe, M., 2015. Tree mortality from drought, insects, and their interactions in a changing climate. New Phytol. 208 (3), 674–683. https://doi.org/10.1111/nph.13477.

Armesto, J.J., Manuschevich, D., Mora, A., Smith-Ramirez, C., Rozzi, R., Abarzúa, A.M., Marquet, P.A., 2010. From the Holocene to the Anthropocene: A historical framework for land cover change in southwestern South America in the past 15,000 years. Land Use Policy 27, 148–160. https://doi.org/10.1016/j.landusepol.2009.07.006.

Arneth, A., Kelliher, F., McSeveny, T., Byers, J., 1998. Ecosystem productivity, net primary productivity and ecosystem carbon sequestration in a *Pinus radiata* plantation subject to soil water deficit. Tree Physiol. 18, 785–793. https://doi.org/10.1093/treephys/18.12.785.

Arnold, J.G., Kiniry, J.R., Srinivasan, R., Williams, J.R., Haney, E.B., Neitsch, S.L. 2012. Soil & Water Assessment Tool: Input/output documentation. Texas Water Resources Institute, TR-439.

Barrientos, G., Iroumé, A., 2018. The effects of topography and forest management on water storage in catchments in south-central Chile. Hydrol. Process. 32 (21), 3225–3240. https://doi.org/10.1002/hyp.13261.

Boisier, J.P., Alvarez-Garretón, C., Cordero, R.R., Damiani, A., Gallardo, L., Garreaud, R. D., Lambert, F., Ramallo, C., Rojas, M., Rondanelli, R., 2018. Anthropogenic drying in central-southern Chile evidenced by long-term observations and climate model simulations. Elem. Sci. Anth. 6 (1), 74. https://doi.org/10.1525/elementa.328.

Bowman, D.M.J.S., Moreira-Muñoz, A., Kolden, C.A., Chávez, R.O., Muñoz, A.A., Salinas, F., Johnston, F.H., 2019. Human–environmental drivers and impacts of the globally extreme 2017 Chilean fires. Ambio 48 (4), 350–362. https://doi.org/10.1007/s13280-018-1084-1.

Bown, H.E., Fuentes, J.P., Martínez, A.M., 2018. Assessing water use and soil water balance of planted native tree species under strong water limitations in Northern Chile. New Forest. 49, 871–892. https://doi.org/10.1007/s11056-018-9689-6.

Bozkurt, D., Rojas, M., Boisier, J.P., Valdivieso, J., 2018. Projected hydroclimate changes over Andean basins in central Chile from downscaled CMIP5 models under the low and high emission scenarios. Clim. Change 150 (3–4), 131–147. https://doi.org/10.1007/s10584-018-2246-7.

Brown, S.C., Versace, V.L., Lester, R.E., Todd Walter, M., 2015. Assessing the impact of drought and forestry on streamflows in south-eastern Australia using a physically based hydrological model. Environ. Earth Sci. 74 (7), 6047–6063. https://doi.org/10.1007/s12665-015-4628-8.

Buttle, J.M., 2011. Streamflow response to headwater reforestation in the Ganaraska River basin, southern Ontario, Canada. Hydrol. Processes 25 (19), 3030–3041. https://doi-org.uchile.idm.oclc.org/10.1002/hyp.8061.

Calder, I.R., 2007. Forests and water-ensuring forest benefits outweigh water costs. For. Ecol. Manage. 251 (1–2), 110–120. https://doi.org/10.1016/j.foreco.2007.06.015.

Carvalho-Santos, C., Nunes, J.P., Monteiro, A.T., Hein, L., Honrado, J.P., 2016. Assessing the effects of land cover and future climate conditions on the provision of

hydrological services in a medium-sized watershed of Portugal. Hydrol. Process. 30 (5), 720–738. https://doi.org/10.1002/hyp.10621.
Chen, L., Wang, G., Zhong, Y., Zhao, X., Shen, Z., 2016. Using site-specific soil samples as a substitution for improved hydrological and nonpoint source predictions. Environ. Sci. Pollut. Res. 23 (16), 16037–16046. https://doi.org/10.1007/s11356-016-6789-8.
Chuvieco, E. 2008. Teledetección ambiental: la observación de la tierra desde el espacio. 3ra ed. Barcelona, España: Ariel Ciencias. 594p. (ISBN 978-8434434981).
Centro de Información de los Recursos Naturales (CIREN). (1997). Descripciones de Suelos Materiales y Simbolo: Estudio agrologico VII Región. ISBN Obra Completa 956 - 7153 - 36 – 1.
Centro de Información de los Recursos Naturales (CIREN). 2001. Cartografía Propiedades rurales. Esc. 1: 10.000.
Collins, M., Knutti, R., Arblaster, J., Dufresne, J.-L., Fichefet, T., Friedlingstein, P., Gao, X., Gutowski, W.J., Johns, T., Krinner, G., Shongwe, M., Tebaldi, C., Weaver, A.J., Wehner, M. 2013. Long-term Climate Change: Projections, Commitments and Irreversibility. In: Climate Change 2013: The Physical Science Basis. Contribution of Working Group I to the Fifth Assessment Report of the Intergovernmental Panel on Climate Change [Stocker, T.F., D. Qin, G.-K. Plattner, M. Tignor, S.K. Allen, J. Boschung, A. Nauels, Y. Xia, V. Bex and P.M. Midgley (eds.)]. Cambridge University Press, Cambridge, United Kingdom and New York, NY, USA.
Devia, G.K., Ganasri, B.P., Dwarakish, G.S., 2015. A review on hydrological models. Aquat. Procedia 4, 1001–1007. https://doi.org/10.1016/j.aqpro.2015.02.126.
Dile, Y.T., Daggupati, P., George, C., Srinivasan, R., Arnold, J., 2016. Introducing a new open source GIS user interface for the SWAT model. Environ. Modell. Softw. 85, 129–138. https://doi.org/10.1016/j.envsoft.2016.08.004.
Echeverria, C., Coomes, D., Salas, J., Rey-Benayas, J.M., Lara, A., Newton, A., 2006. Rapid deforestation and fragmentation of Chilean temperate forests. Biol. Conserv. 130 (4), 481–494. https://doi.org/10.1016/j.biocon.2006.01.017.
Estay, S.A., Chávez, R.O., Rocco, R., Gutiérrez, A.G., 2019. Quantifying massive outbreaks of the defoliator moth *Ormiscodes amphimone* in deciduous *Nothofagus*-dominated southern forests using remote sensing time series analysis. J. Appl. Entomol. 143, 787–796. https://doi.org/10.1111/jen.12643.
Falvey, M., Garreaud, R.D., 2009. Regional cooling in a warming world: Recent temperature trends in the southeast Pacific and along the west coast of subtropical South America (1979–2006). J. Geophys. Res. 114 (4), D04102. https://doi.org/10.1029/2008JD010519.
Farley, K.A., Jobbágy, E.G., Jackson, R.B., 2005. Effects of afforestation on water yield: A global synthesis with implications for policy. Glob. Change Biol. 11 (10), 1565–1576. https://doi.org/10.1111/j.1365-2486.2005.01011.x.
Ferraz, S.F.B., Rodriguez, C.B., Garcia, L.G., Alvares, A.A., Lima, W.D.P., Rodrigues, C.B., Lima, W.D.P., 2019. Effects of Eucalyptus plantations on streamflow in Brazil: Moving beyond the water use debate. For. Ecol. Manage. 453 https://doi.org/10.1016/j.foreco.2019.117571676.
Filoso, S., Bezerra, M.O., Weiss, K.C.B., Palmer, M.A., 2017. Impacts of forest restoration on water yield: A systematic review. PLoS One 12 (8), e0183210. https://doi.org/10.1371/journal.pone.0183210.
Gallo, E.L., Meixner, T., Aoubid, H., Lohse, K.A., Brooks, P.D., 2015. Combined impact of catchment size, land cover, and precipitation on streamflow and total dissolved nitrogen: A global comparative analysis. Global Biogeochem. Cycles 29 (7), 1109–1121. https://doi.org/10.1002/2015GB005154.
Garmendia, E., Mariel, P., Tamayo, I., Aizpuru, I., Zabaleta, A., 2012. Assessing the effect of alternative land uses in the provision of water resources: Evidence and policy implications from southern Europe. Land Use Policy 29 (4), 761–770. https://doi.org/10.1016/j.landusepol.2011.12.001.
Garreaud, R.D., Alvarez-Garreton, C., Barichivich, J., Pablo Boisier, J., Christie, D., Galleguillos, M., LeQuesne, C., McPhee, J., Zambrano-Bigiarini, M., 2017. The 2010–2015 megadrought in central Chile: Impacts on regional hydroclimate and vegetation. Hydrol. Earth Syst. Sci. 21 (12), 6307–6327. https://doi.org/10.5194/hess-21-6307-2017.
Garreaud, R., Falvey, M., Montecinos, A., 2016. Orographic precipitation in coastal Southern Chile: Mean distribution, temporal variability, and linear contribution. J. Hydrometeorol. 17 (4), 1185–1202. https://doi.org/10.1175/jhm-d-15-0170.1.
Gassman, P.W., Sadeghi, A.M., Srinivasan, R., 2014. Applications of the SWAT model special section: Overview and insights. J. Environ. Qual. 43, 1–8. https://doi.org/10.2134/jeq2013.11.0466.
Government of Chile. 2020. Chile's Nationally Determined Contribution, update 2020. Council of Ministers for Sustainability. Available online: https://www4.unfccc.int/sites/ndcstaging/PublishedDocuments/Chile%20First/, (accessed on 23 April 2020).
Guada, G., Camarero, J.J., Sánchez-Salguero, R., Cerrillo, R.M.N., 2016. Limited growth recovery after drought-induced forest dieback in very defoliated trees of two pine species. Front. Plant Sci. 7 (April), 1–12. https://doi.org/10.3389/fpls.2016.00418.
Heathman, G.C., Larose, M., Cosh, M.H., Bindlish, R., 2009. Surface and profile soil moisture spatio-temporal analysis during an excessive rainfall period in the Southern Great Plains, USA. CATENA 78, 159–169. https://doi.org/10.1016/j.catena.2009.04.002.
Hengl, T., De Jesus, J.M., Heuvelink, G.B.M., Gonzalez, M.R., Kilibarda, M., Blagotić, A., Kempen, B., 2017. SoilGrids250m: Global gridded soil information based on machine learning. PLoS One 12. https://doi.org/10.1371/journal.pone.0169748.
Huang, S., Zheng, X., Ma, L., Wang, H., Huang, Q., Leng, G., Guo, Y., 2020. Quantitative contribution of climate change and human activities to vegetation cover variations based on GA-SVM model. J. Hydrol. 124687 https://doi.org/10.1016/j.jhydrol.2020.124687.
Huber, J.A., Trecaman, V.R., 2004. Eficiencia del uso del agua en plantaciones de Pinus radiata en Chile. Bosque (Valdivia) 25 (3), 33–43. https://doi.org/10.4067/s0717-92002004000300004.
Huber, A., Iroume, A., Bathurst, J., 2008. Effect of Pinus radiata plantations on water balance in Chile. Hydrol. Process. 22, 142–148. https://doi.org/10.1002/hyp.6582.
Huber, A., Iroume, A., Mohr, C., Frene, C., 2010. Effect of Pinus radiata and Eucalyptus globulus plantations on water resource in the Coastal Range of Biobio region, Chile. Bosque 31 (3), 219–230. https://doi.org/10.4067/S0717-92002010000300006.
Instituto Nacional Forestal (INFOR). 2015. Los recursos forestales en Chile: Inventario continuo de bosques nativos y actualización de plantaciones forestales. https://bibliotecadigital.infor.cl/handle/20.500.12220/21002.
IPCC, (2013): Annex I: Atlas of Global and Regional Climate Projections [van Oldenborgh, G.J., M. Collins, J. Arblaster, J.H. Christensen, J. Marotzke, S.B. Power, M. Rummukainen and T. Zhou (eds.)]. In: Climate Change 2013: The Physical Science Basis. Contribution of Working Group I to the Fifth Assessment Report of the Intergovernmental Panel on Climate Change [Stocker, T.F., D. Qin, G.-K. Plattner, M. Tignor, S.K. Allen, J. Boschung, A. Nauels, Y. Xia, V. Bex and P.M. Midgley (eds.)]. Cambridge University Press, Cambridge, United Kingdom and New York, NY, USA.
Iroumé, A., Palacios, H., 2013. Afforestation and changes in forest composition affect runoff in large river basins with pluvial regime and Mediterranean climate, Chile. J. Hydrol. 505, 113–125. https://doi.org/10.1016/j.jhydrol.2013.09.031.
Jones, J., Almeida, A., Cisneros, F., Iroumé, A., Jobbágy, E., Lara, A., Villegas, J.C., 2016. Forests and water in South America. Hydrol. Process. 31 (5), 972–980. https://doi.org/10.1002/hyp.11035.
Jürgensen, C., Kollert, W., & Lebedys, A. (2014). Assessment of industrial roundwood production from planted forests. FAO Planted Forests and Trees Working Paper FP/48/E. www.fao.org/forestry/plantedforests/67508@170537/en/.
Landis, J.R., Koch, G.G., 1977. The measurement of observer agreement for categorical data. Retrieved from Biometrics 33 (1), 159–174. www.ncbi.nlm.nih.gov/pubmed/843571.
Lara, A., Veblen, T., 1993. Forest plantations in Chile: a successful model? In: Mather, A. (Ed.), Afforestation. Belhaven Press, United Kingdom, pp. 118–139.
Lara, A., Little, C., Urrutia, R., McPhee, J., Álvarez-Garretón, C., Oyarzún, C., Arismendi, I., 2009. Assessment of ecosystem services as an opportunity for the conservation and management of native forests in Chile. For. Ecol. Manage. 258 (4), 415–424. https://doi.org/10.1016/j.foreco.2009.01.004.
Lara, A., Little, C., González, M., Lobos, D. 2013. Restauración de bosques nativos para aumentar la provisión de agua como un servicio ecosistémico en el centro-sur de Chile: desde las pequeñas cuencas a la escala de paisaje. Pp 57-78 En: Lara A., P Laterra, R Manson, G Barrantes. (eds.). Servicios ecosistémicos hídricos: estudios de caso en América Latina y el Caribe. Red ProAgua CYTED. Valdivia, Chile. Imprenta América. 316p.
Liew, M.W.V., Veith, T., Bosch, D., Arnold, J.G., 2007. Suitability of SWAT for the conservation effects assessment project: A comparison on USDA-ARS experimental watersheds. J. Hydrol. Eng. 12 (2), 173–189. https://doi.org/10.1061/(ASCE)1084-0699(2007)12:2(173).
Little, C., Lara, A., McPhee, J., Urrutia, R., 2009. Revealing the impact of forest exotic plantations on water yield in large scale watersheds in South-Central Chile. J. Hydrol. 374, 162–170. https://doi.org/10.1016/j.jhydrol.2009.06.011.
Little, C., y Lara, A., 2010. Restauración ecológica para aumentar la provisión de agua como un servicio ecosistémico en cuencas forestales del centro-sur de Chile. Bosque 31, 175–178. https://doi.org/10.4067/S0717-92002010000300001.
Lu, Z., Zou, S., Qin, Z., Yang, Y., Xiao, H., Wei, Y., Xie, J., 2015. Hydrologic responses to land use change in the Loess Plateau: Case study in the Upper Fenhe River Watershed. Adv. Meteorol. 2015, 1–10. https://doi.org/10.1155/2015/676030.
Luebert, F., y Pliscoff, P. 2018. Sinopsis bioclimática y vegetacional de Chile. Segunda edición. Editorial Universitaria, Santiago. www.uchile.cl/publicaciones/141285/sinopsis-bioclimatica-y-vegetacional-de-chile.
Manuschevich, D., Sarricolea, P., Galleguillos, M., 2019. Integrating socio-ecological dynamics into land use policy outcomes: A spatial scenario approach for native forest conservation in south-central Chile. Land Use Policy 84, 31–42. https://doi.org/10.1016/j.landusepol.2019.01.042.
Mcvicar, T.R., Roderick, M.L., Donohue, R.J., Van Niel, T.G., 2012. Less bluster ahead? ecohydrological implications of global trends of terrestrial near-surface wind speeds. Ecohydrology 5 (4), 381–388. https://doi.org/10.1002/eco.1298.
Meza, F.J., Montes, C., Bravo-Martínez, F., Serrano-Ortiz, P., Kowalski, A.S., 2018. Soil water content effects on net ecosystem CO2 exchange and actual evapotranspiration in a Mediterranean semiarid savanna of Central Chile. Sci. Rep. 8 (1), 1–11. https://doi.org/10.1038/s41598-018-26934-z.
Ministerio de Agricultura (MINAGRI). 2015. Política forestal 2015 - 2035. 76p. www.conaf.cl/wp-content/files_mf/1462549405politicaforestal201520351.pdf.
Mishra, S. K., Sahany, S., Salunke, P., Kang, I.-S., & Jain, S. 2018. Fidelity of CMIP5 multi-model mean in assessing Indian monsoon simulations. Npj Clim. Atmos. Sci., 1 (1). https://dx.doi. org/10.1038/s41612-018-0049-1.
Mittermeier, R.A., Robles Gil, P., Hoffman, M., Pilgrim, J., Brooks, T., Mittermeier, C.G., Lamoreux, J., da Fonseca, G.A. 2004. Hotspots Revisited: Earth's Biologically Richest and Most Endangered Terrestrial Ecoregions. Conservation International, CEMEX, Agrupación Sierra Madre, University of Virginia (392 pp.).
Molina-Navarro, E., Hallack-Alegría, M., Martínez-Pérez, S., Ramírez-Hernández, J., Mungaray-Moctezuma, A., Sastre-Merlín, A., 2016. Hydrological modeling and climate change impacts in an agricultural semiarid region. Case study: Guadalupe River basin, Mexico. Agric. Water Manage. 175, 29–42. https://doi.org/10.1016/j.agwat.2015.10.029.
Moriasi, D.N., Arnold, J.G., Van Liew, M.W., Bingner, R.L., Harmel, R.D., Veith, T.L., 2007. Model evaluation guidelines for systematic quantification of accuracy in

watershed simulations. Am. Soc. Agric. Biol. Eng. 50 (3), 885–900. https://doi.org/10.13031/2013.23153.
Neitsch, S. L., Arnold, J. G., Kiniry, J. R., & Williams, J. R. (2011). Soil & Water Assessment Tool Theoretical Documentation Version 2009. Texas Water Resources Institute, 647.
Navarro-Cerrillo, R., Rodriguez-Vallejo, C., Silveiro, E., Hortal, A., Palacios-Rodríguez, G., Duque-Lazo, J., Camarero, J., 2018. Cumulative drought stress leads to a loss of growth resilience and explains higher mortality in planted than in naturally regenerated *Pinus pinaster* stands. Forests 6. https://doi.org/10.3390/f9060358.
Nguyen, H.H., Recknagel, F., Meyer, W., Frizenschaf, J., 2017. Analysing the effects of forest cover and irrigation farm dams on streamflows of water-scarce catchments in South Australia through the SWAT model. Water 9 (1), 1–16. https://doi.org/10.3390/w9010033.
Niklitschek, M.E., 2007. Trade liberalization and land use changes: Explaining the expansion of afforested land in Chile. For. Sci. 53 (3), 385–394.
Ojeda, H., Rubilar, R., Montes, C., Cancino, J., Espinoza, M., 2018. Leaf area and growth of Chilean radiate pine plantations after thinning across a water stress gradient. N. Z. J. For. Sci. 48, 10. https://doi.org/10.1186/s40490-018-0116-8.
Olivera-Guerra, L., Mattar, C., Galleguillos, M., 2014. Estimation of real evapotranspiration and its variation in Mediterranean landscapes of central-southern Chile. Int. J. Appl. Earth Obs. Geoinf. 28 (1), 160–169. https://doi.org/10.1016/j.jag.2013.11.012.
Ovalle, C., Aronson, J., Del Pozo, A., et al., 1990. The espinal: Agroforestry systems of the mediterranean — type climate region of Chile. Agroforest Syst 10, 213–239. https://doi.org/10.1007/BF00122913.
Payn, T., Carnus, J.M., Freer-Smith, P., Kimberley, M., Kollert, W., Liu, S., Wingfield, M. J., 2015. Changes in planted forests and future global implications. For. Ecol. Manage. 352, 57–67. https://doi.org/10.1016/j.foreco.2015.06.021.
Piani, C., Weedon, G.P., Best, M., Gomes, S., Viterbo, P., Hagemann, S., Haerter, J.O., 2010. Statistical bias correction of global simulated daily precipitation and temperature for the application of hydrological models. J. Hydrol. 395, 199–215. https://doi.org/10.1016/j.jhydrol.2010.10.024.
Pilgrim, D.H., Cordery, I., Baron, B.C., 1982. Effects of catchment size on runoff relationships. J. Hydrol. 58 (3–4), 205–221. https://doi.org/10.1016/0022-1694(82)90035-X.
Pino, P., Iglesias, V., Garreaud, R., Cortés, S., Canals, M., Folch, W., Burgos, S., Levy, K., Naeher, L.P., Steenland, K., 2015. Chile confronts its environmental health future after 25 years of accelerated growth. Ann. Glob. Health 81 (3), 354–367. https://doi.org/10.1016/j.aogh.2015.06.008.
Polade, S.D., Gershunov, A., Cayan, D.R., Dettinger, M.D., Pierce, D.W., 2017. Precipitation in a warming world: Assessing projected hydro-climate changes in California and other Mediterranean climate regions. Sci. Rep. 7 (1), 1–10. https://doi.org/10.1038/s41598-017-11285-y.
Putuhena, W.M., Cordery, I., 2000. Some hydrological effects of changing forest cover from eucalypts to Pinus radiata. Agric. For. Meteorol. 100 (1), 59–72. https://doi.org/10.1016/S0168-1923(99)00086-6.
Quilbé, R., Rousseau, A.N., Moquet, J.-S., Trinh, N.B., Dibike, Y., Gachon, P., Chaumont, D., 2008. Assessing the effect of climate change on river flow using general circulation models and hydrological modelling – Application to the Chaudière River, Québec, Canada. Can. Water Resour. J. 33 (1), 73–94. https://doi.org/10.4296/cwrj3301073.
Raab, N., Meza, F.J., Franck, N., Bambach, N., 2015. Empirical stomatal conductance models reveal that the isohydric behavior of an Acacia caven Mediterranean Savannah scales from leaf to ecosystem. Agric. For. Meteorol. 213, 203–216. https://doi.org/10.1016/j.agrformet.2015.06.018.
Rojas, M., Lambert, F., Ramirez-Villegas, J., Challinor, A., 2019. Emergence of robust precipitation changes across crop production areas in the 21st century. PNAS. https://doi.org/10.1073/pnas.1811463116.
Rook, D.A., Corson, M.J., 1978. Temperature and irradiance and the total daily photosynthetic production of the crown of a *Pinus radiata* tree. Oecologia 36, 371–382. https://doi.org/10.1007/BF00348063.
Rossing, T. 2010. Water scarcity, climate change, and the poor. Reducing Poverty, Protecting Livelihoods, and Building Assets in a Changing Climate, 21.
Salas, C., Donoso, P.J., Vargas, R., Arriagada, C.A., Pedraza, R., Soto, D.P., 2016. The forest sector in Chile: An overview and current challenges. J. Forest. 114 (5), 562–571. https://doi.org/10.5849/jof.14-062.
Saltelli, A., Annoni, P., Azzini, I., Campolongo, F., Ratto, M., Tarantola, S., 2010. Variance based sensitivity analysis of model output. Design and estimator for the total sensitivity index. Comput. Phys. Commun. 181 (2), 259–270. https://doi.org/10.1016/j.cpc.2009.09.018.
Sands, R., Nambiar, E.K.S., 1984. Water relations of Pinus radiata in competition with weeds. Can. J. For. Res. 14, 233–237.
Schwalm, C., Glendon, S., Duffy, P., 2020. Rcp8.5 tracks cumulative CO2 emissions. PNAS 117 (33), 19656–19657. https://doi.org/10.1073/pnas.2007117117.
Scott, D.F., Prinsloo, F.W., 2008. Longer-term effects of pine and eucalypt plantations on streamflow. Water Resour. Res. 44, 8. https://doi.org/10.1029/2007WR006781.
Sepulveda, M.M., Bown, H.E., Fernandez, L.B., 2018. Stomatal conductance responses of Acacia caven to seasonal patterns of water availability at different soil depths in a mediterranean savanna. Water 10 (11). https://doi.org/10.3390/w10111534.
Serpa, D., Nunes, J.P., Santos, J., Sampaio, E., Jacinto, R., Veiga, S., Lima, J.C., Moreira, M., Corte-Real, J., Keizer, J.J., Abrantes, N., 2015. Impacts of climate and land use changes on the hydrological and erosion processes of two contrasting Mediterranean catchments. Sci. Total Environ. 538, 64–77. https://doi.org/10.1016/j.scitotenv.2015.08.033.
Sheriff, D.W., Mattay, J.P., McMurtrie, R.E., 1996. Modeling productivity and transpiration of Pinus radiata: Climatic effects. Tree Physiol. 16 (1–2), 183–186. https://doi.org/10.1093/treephys/16.1-2.183.
Sobol, I.M., 2001. Global sensitivity indices for nonlinear mathematical models and their Monte Carlo estimates. Math. Comput. Simul. (MATCOM) 55 (1), 271–280.
Soto, L., Galleguillos, M., Seguel, O., Sotomayor, B., Lara, A., 2019. Assessment of soil physical properties' statuses under different land covers within a landscape dominated by exotic industrial tree plantations in south-central Chile. J. Soil Water Conserv. 74 (1), 12–23. https://doi.org/10.2489/jswc.74.1.12.
Stehr, A., Aguayo, M., Link, O., Parra, O., Romero, F., Alcayaga, H., 2010. Modelling the hydrologic response of a mesoscale Andean watershed to changes in land use patterns for environmental planning. Hydrol. Earth Syst. Sci. 14 (10), 1963–1977. https://doi.org/10.5194/hess-14-1963-2010.
Swann, A., Hoffman, F.D., Koven, C.D., Randerson, J.T., 2016. Plant responses to increasing CO2 reduce estimates of climate impacts on drought severity. PNAS 113 (36), 10019–10024. https://doi.org/10.1073/pnas.1604581113.
Teskey, R., Sheriff, D.W., 1996. Water use by Pinus radiata trees in a plantation. Tree Physiol. 16 (1–2), 273–279. https://doi.org/10.1093/treephys/16.1-2.273.
UN General Assembly, Transforming our world: the 2030 Agenda for Sustainable Development, 21 October 2015, A/RES/70/1, available at: www.refworld.org/docid/57b6e3e44.html.
Valdés-Pineda, R., Pizarro, R., García-Chevesich, P., Valdés, J.B., Olivares, C., Vera, M., Helwig, B., 2014. Water governance in Chile: Availability, management and climate change. J. Hydrol. 519 (PC), 2538–2567. https://doi.org/10.1016/j.jhydrol.2014.04.016.
Xie, Y.Y., Wang, X.J., Silander, J.A., 2015. Deciduous forest responses to temperature, precipitation, and drought imply complex climate change impacts. PNAS 112 (44), 13585–13590. https://doi.org/10.1073/pnas.1509991112.
Yang, Q., Zhang, X., 2016. Improving SWAT for simulating water and carbon fluxes o forest ecosystems. Sci. Total Environ. 569–570, 1478–1488.
Yang, Y., Anderson, M., Gao, F., Hain, C., Noormets, A., Sun, G., Sun, L., 2018. Investigating impacts of drought and disturbance on evapotranspiration over a forested landscape in North Carolina, USA using high spatiotemporal resolution remotely sensed data. Remote Sens. Environ. December, 111018 https://doi.org/10.1016/j.rse.2018.12.017.
Yu, M., Wang, G., Pal, J.S., 2016. Effects of vegetation feedback on future climate change over West Africa. Clim. Dyn. 46, 3669–3688. https://doi.org/10.1007/s00382-015-2795-7.
Zambrano-Bigiarini, M., Rojas, R., 2013. A model-independent particle swarm optimisation software for model calibration. Environ. Modell. Softw. 43, 5–25. https://doi.org/10.1016/j.envsoft.2013.01.004.
Zhang, L., Zhao, F., Chen, Y., Dixon, R.N.M., 2011. Estimating effects of plantation expansion and climate variability on streamflow for catchments in Australia. Water Resour. Res. 47 (12) https://doi.org/10.1029/2011WR010711.
Zhang, M., Liu, N., Harper, R., Li, Q., Liu, K., Wei, X., Liu, S., 2017. A global review on hydrological responses to forest change across multiple spatial scales: Importance of scale, climate, forest type and hydrological regime. J. Hydrol. 546, 44–59. https://doi.org/10.1016/j.jhydrol.2016.12.040.